M 2023

U.PORTO
FEUP FACULDADE DE ENGENHARIA
UNIVERSIDADE DO PORTO

INVESTIGATION OF ANION EXCHANGE MEMBRANE UREA ELECTROLYSIS

EFFECT OF MEMBRANE AND CATALYST ON PERFORMANCE AND AMMONIA PRODUCTION

GUILHERME GIL GONÇALVES CARDOSO DA SILVA

MASTER THESIS IN CHEMICAL ENGINEERING
PRESENTED TO THE FACULTY OF ENGINEERING
OF THE UNIVERSITY OF PORTO

Master in Chemical Engineering

Investigation of anion exchange membrane urea electrolysis: Effect of membrane and catalyst on performance and ammonia production

Master dissertation

of

Guilherme Gil Goncalves Cardoso da Silva

Developed within the course of dissertation

held in

DLR- Deutsches Zentrum für Luft-und Raumfahrt

Supervisor at FEUP: **Prof. Adélio Mendes**

Coordinator at DLR: **Dr. Tobias Morawietz**

August 2023

Acknowledgment

Firstly, I would like to thank Prof. Dr. Adélio Mendes for accompanying the work done with regular meetings, giving plenty of valuable advice and thoughts that serve as guidance.

From DLR, I would like to start to thank Dr. Tobias Morawietz for the supervision, planning, leadership and for the previous knowledge that he has passed through to me about this subject. His enthusiasm for progress in the subject and the insight he brought helped for the work progress. I am also very thankful for the help and guidance from Jagoda Chmielarz who taught me most of standard procedures for test, assembling and the rest of the experimental work and data analysis. Her day-to-day monitoring of my work was crucial.

I would like to thank Prof.Dr.rer.nat. K. Andreas Friedrich, Head of Department Electrochemical Energy Technology Institute of Engineering Thermodynamics, for the opportunity to join such a great research instituition and team leaders for Low Temperature Fuel Cell & Electrolysis Group Leaders Dr.rer.nat. Pawel Gazdzicki and Dr. Aldo Saul Gago Rodriguez.

I am grateful for my journey in DLR and in Stuttgart and for that I thank the rest of DLR members: Vicent Wilke, Jorge Torrero Cámara, Juan Sanchez Monreal, Alvaro Garcia Corral, Abissaid Martínez-Séptimo, Sambal Shashank Ambu, Qingying Zhao, Suryia Venkatesan, Jörg Bürkle and all the other colleagues from the institute. I would also extend thanks to all my fellow students working in DLR, mainly André who came from Porto to Stuttgart as well. Everyone mentioned above helped not only in my work but also made this difficult journey much more enjoyable and their welcoming reception helped on the tougher days.

From University of Porto, I wish to thank Sofia Delgado and Eva Sousa for the electrochemical workshop done before my departure to Stuttgart and the time they gave up. Also, a special word to Professor Luís Miguel Maderia, supervisor of Erasmus+ internsheeps in chemical engineering, for his help in all necessary procedures.

To Moritz Korthals, Carsten Dalacker and everyone at Stuttgarter Rudergesellschaft rowing club that let me train during my stay in Stuttgart and allowed me to continue do a sport that is so dear to me.

To Gonçalo, Guilherme, Rui, Henrique and all other friends, family and teachers who helped me along the way in this last five fantastic years.

Finally, I must thank my mother and my father, who helped me not only financially but also mentally in this big step in my life. I'm forever grateful for their commitment and unconditional support. To my brother for his companionship and his incentive. A very special

thank you to my girlfriend, Gabriela, who helped me every day through highs and lows and supported my decision even if it meant taking us apart for a few months.

This work would not be possible if it wasn't for the funding from Erasmus+ program and from DLR. This work was also financially supported by the Project "Baterias 2030" with the reference POCI-01-0247-FEDER-046846, co-financed by the Competitiveness and Internationalisation Operational Programme (COMPETE 2020), within the Partnership Agreement - Portugal 2020, through the European Regional Development Fund (ERDF).

Abstract

Nitrogen oxides (NOx) are one of the most dangerous anthropogenic forms of pollution known. NOx can cause health hazards linked to respiratory and cardiovascular systems. NOx emissions can also contribute to the formation of tropospheric ozone, acid rain, and depletion of the ozone layer. In this work, an innovative H2-deNOx technology, that would complement the selective catalytic reduction (SRC) technology, is studied for NOx abatement in mobility applications. The H2-deNOx approach could help diesel engines to comply with the strict regulation for NOx emissions that have been implemented in the EU over the years. This approach enables high efficiencies of NOx removal from the engine exhaust gas even in cold conditions, where SCR tends to fail.

Anion exchange membrane electrolysis, a promising and emerging technology for electrochemical water splitting, was adapted for the conversion of an aqueous solution of urea, AdBlue, into ammonia and hydrogen (eU2A). These gases are subsequently used for the reduction of NOx in the exhaust gas stream. The influence of several components that compose this electrochemical device are studied. The influence of operating conditions such as temperature and potassium hydroxide (KOH) concentrations are investigated. Three main experimental tests were used: a) rotating disk electrode (RDE) was performed to provide insights into the electrocatalytic activity in the anodic reaction (oxygen and ammonia production); b) submerged cells and c) closed electrolyzer cells were used for MEA characterization – in submerged cells different KOH concentrations and temperatures were used while in closed cells, catalyst coating techniques (like CCM and CCS) were the focal point.

It was concluded that the current density of the electrochemical conversion of urea into ammonia by AEM electrolysis is low and needs to be increased. With pure AdBlue, current densities of 70 mA cm^{-2} were obtained for submerged cells at 2 V, while using the RDE anodic reaction this value was 3 mA cm^{-2}, at 1.8 V. Adding 1 M KOH improves drastically the current density, reaching 300 mA cm^{-2} in submerged cells at 2 V, 125 mA cm^{-2} in RDE at 1.8 V and almost 500 mA cm^{-2} at 2 V in closed electrolyzer cell; though much higher than without supporting electrolyte, this approach still underperforming for making the technology commercial. The relatively low current density was assigned to the poor electric conductivity and poor mass transport kinetics of the urea solution. Besides increasing the current density, for making the H2-deNOx technology commercial, it should also be addressed the stability of the anion exchange membranes used.

Keywords: eU2A, AEMWE, Electrolysis, AdBlue, DeNOx.

Resumo

Os óxidos de azoto (NOx) são uma das formas mais perigosas de poluição antropogénica conhecidas. O NOx pode causar riscos para a saúde relacionados com os sistemas respiratório e cardiovascular. As emissões de NOx também podem contribuir para a formação de ozono troposférico, chuva ácida e diminuição da camada de ozono. Neste trabalho, é estudada uma tecnologia inovadora, H2-deNOx, que poderá complementar a tecnologia de redução catalítica seletiva (SCR) para a redução de NOx em aplicações de mobilidade. A abordagem H2-deNOx pode ajudar os motores a diesel a cumprir as rigorosas regulamentações de emissões de NOx que foram implementadas na UE ao longo dos anos. Esta abordagem permite elevadas eficiências na remoção de NOx dos gases de escape do motor, mesmo em condições frias, onde o SRC tende a falhar.

A eletrólise de membrana de permuta aniónica, uma tecnologia promissora e emergente para a decomposição eletroquímica da água, foi adaptada para a conversão de uma solução aquosa de ureia, AdBlue, em amoníaco e hidrogénio (eU2A). Estes gases são posteriormente utilizados para a redução de NOx na corrente de gases de escape. É estudada a influência de vários componentes que compõem este dispositivo eletroquímico. Investigam-se as influências das condições de operação, como a temperatura e concentrações de hidróxido de potássio (KOH). Foram realizados três principais testes experimentais: a) elétrodo de disco rotativo (RDE) foi utilizado para fornecer informações sobre a atividade eletrocatalítica na reação anódica (produção de oxigénio e amoníaco); b) células submersas e c) células eletrolisadoras fechadas foram utilizadas para caracterização de MEAs - em células submersas, diferentes concentrações de KOH e temperaturas foram utilizadas, enquanto que nas células fechadas, as técnicas de deposição do catalisador (CCM e CCS) foram o foco principal.

Concluiu-se que a densidade de corrente da conversão eletroquímica da ureia em amoníaco por eletrólise de membrana de permuta aniónica é baixa e precisa de ser aumentada. Com AdBlue puro, foram obtidas densidades de corrente de 70 $mA \cdot cm^{-2}$ em células submersas a 2 V, enquanto que no dispositivo RDE, o valor obtido foi de 3 $mA \cdot cm^{-2}$, a 1.8 V. A adição de 1 M de KOH melhora drasticamente a densidade de corrente, atingindo 300 $mA \cdot cm^{-2}$ em células submersas a 2 V, 125 $mA \cdot cm^{-2}$ em RDE a 1,8 V e quase 500 $mA \cdot cm^{-2}$ em células eletrolisadoras fechadas a 2 V; embora seja muito maior do que sem eletrólito de suporte, esta abordagem ainda não atinge o desempenho necessário para tornar a tecnologia comercial. A densidade de corrente relativamente baixa foi atribuída à baixa condutividade elétrica e ao mau transporte de massa da solução de ureia. Além de aumentar a densidade de corrente, para tornar a tecnologia H2-deNOx comercial, também é necessário abordar a estabilidade das membranas de permuta aniónica utilizadas.

Declaration

I hereby declare, under word of honour, that this work is original and that all non-original contributions is indicated and due reference is given to the author and source

Guilherme Gil Gonçalves Cardoso da Silva

Porto, 2nd of August 2023

Index

1 Introduction 1

1.1 Framing and presentation of the work 1

1.2 Presentation of the company 3

1.3 Contribution of the author to the work 3

1.4 Organization of the dissertation 4

2 Context and State of the art 5

2.1 Diesel Engines and reduction of emissions 5

2.1.1 Ammonia-Selective Catalytic Reaction 6

2.1.2 Urea to ammonia conversion 6

2.1.3 Hydrogen deNOx (H2-deNOx) 8

2.2 Anion Exchange Membrane Water Electrolysis 9

2.2.1 Anion Exchange Membrane 10

2.2.2 Hydrogen Evolution Reaction and Oxygen Evolution Reaction catalysts 11

2.2.3 Membrane Electrode Assembly 14

2.2.4 Operating Conditions and other components 16

2.3 Urea-assisted Water electrolysis 17

3 Materials and Methods 19

3.1 Submerged Cells 19

3.2 RDE 21

3.3 Continuous flow cells 23

4 Results and discussion 25

4.1 Rotating Disk Electrode 25

4.1.1 Ink and deposition Optimization 25

4.1.2 Catalyst performance 26

4.1.3 UPW and KOH *vs* AdBlue and KOH 28

4.2 Submerged Cells 29

4.2.1 Temperature 29

4.2.2 MEA 30
4.2.3 KOH concentrations in AdBlue *vs* in UPW 31
4.2.4 Electrochemical Impedance Spectroscopy 33
4.3 Closed Cell 35
4.3.1 Torque and Flow rate optimization 35
4.3.2 KOH Influence 36
4.3.3 CCM *vs* CCS *vs* CCM-CCS 37
5 Conclusion 39
6 Assessment of the work done 41
6.1 Objectives Achieved 41
6.2 Final Assessment 41
7 References 43
Annex A - Urea Full Oxidation- Intermediate Steps 49
Appendice A Commercially Available Anion Exchange Membranes 51
Appendice B Nitrogen (N_2) and Oxygen (O_2) purge 53

List of Figures

Figure 2.1-Representation of exhaust-gas after treatment in a diesel car- adapted[14, 15]. 6

Figure 2.2- Electrolytic cell for production of ammonia and hydrogen, extracted from [21]..... 7

Figure 2.3- Exhaust gas treatment with H_2-DeNOx treatment and decoupled Urea decomposition..... 8

Figure 3.1- Representation of submerged cell setup, taken and adapted from Xu et al. [74]..... 19

Figure 3.2- Apparatus for RDE experimental tests and closer look into Electrodes used 22

Figure 3.3-a) Example of a catalytic Ink used during RDE experiments, with OXYGEN-N..... 22

Figure 3.4- Closed Cell test bench with anode on the left and cathode on the right 23

Figure 4.1- OXYGEN-N inks developed for RDE measurement. First ink prepared and optimized one on the left and right, respectively..... 25

Figure 4.2-RDE measurements in different electrolytes, studied at room temperature (ca. 20 °C-25 °C). a) and b) are corrected and uncorrected results in pure AdBlue, respectively. c) and d) are the corrected and uncorrected results in AdBlue+1 M KOH, respectively and e) and f) are the corrected and uncorrected results in UPW+1 M KOH, respectively. 27

Figure 4.3- RDE measurements for OXYGEN-N, different support electrolytes at room temperature (20 °C-25 °C), a) is the uncorrected plot and b) already corrected 28

Figure 4.4- Temperature influence on AdBlue electrolysis for a) SC.4, Sustanion MEA, in Pure AdBlue ; b) SC.6, experimental MEA in AdBlue and 1M KOH 29

Figure 4.5- a) and b) show the results for 3 different membranes used in MEA (SC 3,5 and 8). a) is at 70 °C AdBlue and b) is AdBlue with 0.1M KOH at 60 °C 30

Figure 4.6- SC.6 MEA, tested in AdBlue with different KOH concentrations, at 70 °C..... 31

Figure 4.7- comparison between AdBlue and UPW supporting electrolyte with 0.1M KOH. SC.1 and SC.2, with PiperION MEAs used at 50 °C and 60 °C..... 32

Figure 4.8-KOH Concentration comparison for SC.2 in UPW+1 M KOH at 60 °C 33

Figure 4.9- EIS displayed as Nyquist plot; In a) curves were obtained at 1 M KOH in AdBlue for SC.6; in b) temperature used was 70 °C SC.6 and c) comparison at 70 °C for SC.3 and SC.4. 35

Figure 4.10-a) optimization of torque used for submerged cell compression; b) optimization of the cathode flow rate. Measurements done at 60 °C and 2 $mL \cdot min^{-1}$ anode flow rate..... 36

Figure 4.11- Comparison between performances of two closed continuous cells in AdBlue with different KOH concentrations. In a), CC.1 (experimental CCS) was used and b) CC.3 (CCM-Fumatech). Tests run at 60 °C, 40 and 2 $mL \cdot min^{-1}$ flow for cathode and anode respectively..... 37

Figure 4.12- Comparison between MEA coating technique, in AdBlue with 1 M KOH at the operating conditions previously mentioned. 37

Figure B.1-RDE measurements with support electrolyte solutions purged with either O_2 or N_2. In a), pure AdBlue was used and b) used AdBlue+1 M KOH, both at room temperature 53

List of Tables

Table 2.1-SWOT analysis on AEMWE-based on Guilbert et al. and Zakaria et al. 10

Table 3.1- Catalysts used during this work 19

Table 3.2- Cells used during submerged cell testing and their specifications 20

Table 3.3- Cells used during testing in closed cell and their specifications 24

Table 7.1- Sum of Free Energies for All the intermediate Steps, adapted from [22] 49

Table A.1- Commercially Available Anion Exchange Membranes, properties and prices. Some information is undisclosed. Adapted from [76] 51

Notation and Glossary

A	area	m^2

Greek Letters

η	Overpotential	mV

Indexes

i	Current Density	$A \cdot cm^{-2}$
I	Current	A
R	Resistance	Ω
U	Potential	V
U_{cor}	Corrected Potential	V

List of Acronyms

AEI	Anion Exchange Ionomer
AEMWE	Anion Exchange Membrane Water Electrolysis
AWE	Alkaline Water Electrolysis
BPP	Bipolar Plate
CCM	Catalyst Coated Membrane
CCS	Catalyst Coated Substrate
eU2A	Electrochemical Conversion of Urea to Ammonia
HER	Hydrogen Evolution Reaction
IPA	Isopropanol
NOx	Nitrogen Oxides
OER	Oxygen Evolution Reaction
PEMWE	Proton Exchange Membrane Water Electrolysis
PTL	Porous Transport Layer
RDE	Rotating Disk Electrode
SCR	Selective Catalytic Reduction
SS	Stainless Steel
UOR	Urea Oxygen Reaction
UPW	Ultra-Pure Water

1 Introduction

1.1 Framing and presentation of the work

Diesel engines have been used in a wide range of commercial applications, but it is mostly known for their supremacy in the transportation sector, mainly light and heavy-duty trucks. Its superior thermal efficiency, reliability and lower cost contribute to its dominance in the sector. However, diesel cars have been a major source of air pollution in many parts of the world, including Europe. The exhaust emissions from diesel vehicles contain a variety of pollutants, namely CO, nitrogen oxides (NOx), particulate matter (PM), and greenhouse gas CO_2. NOx pollution is one of the main causes of acid rain, tropospheric ozone, depletion of the ozone layer and has a very worrying effect on cardiovascular and respiratory health [1];it is estimated that NO_2 pollution is responsible for 4 million new pediatric asthma cases annually, which accounts for 6 % - 13 % of global incidence [2].

To mitigate exhaust emissions from diesel vehicles, the European Union (EU) has implemented a series of laws and regulations aimed at reducing these emissions. The Euro emissions standards have been progressively tightened over the years, with each new standard requiring a significant reduction in emissions. Euro emission standards-Euro 6 and Euro 7 set very strict limits on NOx and particle matter emissions from diesel cars [3]. The Euro emissions standards and the associated emissions control technologies have helped to significantly reduce the emissions from diesel cars in Europe [4].

To comply with these standards, diesel car manufacturers have implemented a variety of emissions control technologies, including diesel oxidation catalysts (DOC), diesel particulate filters (DPFs), selective catalytic reduction (SCR) systems, and exhaust gas recirculation (EGR) systems. Amid these technologies, SCR system uses a reducing agent such as ammonia to convert NOx into harmless nitrogen and water. Because ammonia is considered toxic, urea ($CO(NH_2)_2$) (normally in an aqueous solution known as AdBlue) is normally used as a storage intermediary that is then hydrolyzed to produce ammonia. Exhaust gas recirculation, on the other hand, recirculates a portion of the exhaust gas back into the engine to reduce the formation of NOx [5]. Typically, several of these technologies are combined to meet the EURO emission requirements.

Despite these improvements, concerns remain about the real-world emissions performance of some diesel cars, particularly in urban areas where air quality is a major concern. As a result, the EU is reviewing and updating the emissions regulations to further reduce emissions from

diesel cars and improve air quality. New technologies and improvements are currently being developed. One promising technology for NOx reduction is the use of not only ammonia but also hydrogen (H_2-deNOx) to complement NOx reduction at lower temperatures.

The present work was developed at DLR – Deutsches Zentrum für Luft- und Raumfahrt with close collaboration to University of Stuttgart, within a comprehensive project, H_2-deNOX 2, for improved reduction of the NOx emissions from diesel cars. The new approach is expected to be more versatile and efficient than the current technology of SCR. The main objective is to develop an AEM electrolyzer where both H_2 and NH_3 are produced while sustaining high current densities and lower stability issues. Testing of small-scale electrolyzers cells took place with different materials, catalysts, membranes/ionomers, and operation conditions. The technology will be based on an AEMWE device for hydrogen production from water (pure water or in alkaline electrolyte) and electrochemical conversion of urea to ammonia (eU2A).

For the past few decades, the development of green hydrogen production solutions got a lot of attention and funding due to its foreseeable importance for a less polluted energy sector. There are several electrolyzer technologies, each with their own advantages and drawbacks. Alkaline and proton exchange membrane water electrolysis (AWE and PEMWE, respectively) are the most mature and used processes for producing green H_2 (respectively, ca. 60 % and 30 % of the share market) [6]. There are also other emerging technologies, such as solid oxide electrolysis cells (SOEC) and anion exchange membrane electrolysis (AEMWE), with the latter aiming to combine the best features of AWE and PEMWE technologies.

The working principle of AEMWE is similar to most of the other electrolysis technologies: water is electrochemically split to form hydrogen and oxygen. Water is reduced at the cathode, resulting in H_2 and hydroxide ions (OH^-) production. These ions migrate then through the membrane to the anode. At the anode, O_2 and water are produced. This technology is similar to PEMWE, since both technologies use an ion exchange membrane – a solid electrolyte that divides the anode from the cathode. However, AEM electrolyzers use non-precious metal catalysts, which reduce the cost and increase the sustainability of the system. They also have the potential to operate at higher current densities than AWE and use lower-grade water; for example, AEM electrolyzers can directly use seawater as a feed solution. There are, however, challenges associated with AEM electrolyzers, such as the stability of the membrane in alkaline conditions, the use of stable catalysts for commercial applications, and most importantly, achieving current densities in the range or above PEMWE.

Using AEM devices for electrochemical reactions with other reactants beside water, is also a promising pathway. In AWE, urea-assisted water electrolysis has gained some notoriety and

can be seen as a viable future alternative to water-only electrolysis. With the urea oxidation reaction (UOR) replacing oxygen evolution reaction (OER), the required potential decreases from 1.23 V *vs* RHE to 0.46 V *vs* RHE [7]. This can mean higher current densities at much lower potentials if other limiting factors are solved.

Electrochemical urea to ammonia (eU2A) conversion differs from urea assisted water electrolysis because instead of complete urea oxidation, only hydrolysis until ammonia production is intended. With AdBlue (mixture of urea and water) and use of an electrolyte like KOH, production of NH_3 and O_2 on the anode and H_2 on the cathode can be achieved. Few studies for eU2A are known and no other experiments with AEM and AdBlue are available. This limits the previous knowledge that can be used for this work and so different catalysts, membranes and components are studied specifically for this purpose. The first approach is done with materials already known to work for AEMWE and urea oxidation but what works in these cases does not necessarily work for eU2A. A balance between cell performance (current density and long-term stability) and ammonia and hydrogen production needs to be achieved.

1.2 Presentation of the company

Deutsches Zentrum für Luft- und Raumfahrt (DLR) or in its English form, German Aerospace Center, is the Federal Republic of Germany's research centre for aeronautics and space. DLR conducts research and development activities in the fields of aeronautics, space, energy, transport, security and digitalisation. DLR uses the expertise of more than 55 research institutes and facilities to develop solutions to the challenges in the fields previously mentioned. DLR's mission is to explore Earth and space and develop technologies for a sustainable future. In doing so, DLR contributes to strengthening Germany's position as a prime location for research and industry. This work was developed in Institut für Technische Thermodynamik (Institute of Engineering Thermodynamics) in Stuttgart, for the Electrochemical Energy Storage Department. This institute does research in the field of efficient energy storage systems that conserve natural resources, and next generation energy conversion technologies. The spectrum of activities ranges from theoretical studies to laboratory work for basic research and to the operation of pilot plants. These experimental and theoretical studies are accompanied by systems analysis studies to analyze the associated technological, environmental, and economic potential and situate it in a larger overall context of the energy economy by means of scenarios.

1.3 Contribution of the author to the work

My contribution to this work was mainly experimental. Conceptually, most of the experiences, test benches, and experimental facilities were already built and used. Besides the rotating disk electrode (RDE) protocol, all other protocols used were previously established in

the project by Ms. Jagoda Chmielarz. RDE protocol, on the other hand, was developed by me, based on a previous one developed by Dr. Tobias Morawietz. Catalyst coated substrates and membranes (CCS and CCM, respectively) were mainly prepared by other lab assistant researchers, while the ink and electrodes preparation for RDE was developed by me.

1.4 Organization of the dissertation

This dissertation contains a dense Context and State of the Art chapter, where very different technologies and subjects are analyzed: from NOx emission reduction technologies in diesel engines to water electrolysis to some up-and-coming technologies such as AEMWE and H2-deNOx. In fact, a brief AEMWE state-of-the-art of all components is comprised for a better understanding of the current R&D status. In this chapter, a concise analysis of urea-assisted water electrolysis is done. It is important to stress that similar technologies for urea to ammonia electrochemical conversion, from AdBlue, are very scarce and inexistent using AEMWE technology to the author's best knowledge.

The third chapter will present the methods and materials for several testing procedures used in this work. Materials used in both submerged cells and continuous closed cells are listed and explained in detail as well as everything used during performance tests. Regarding RDE, all materials used are listed, as well as ink and electrode preparation procedures and testing protocols.

Fourth chapter, “Results and Discussion” will have 3 subchapters where all 3 technologies used and the results obtained are displayed and analyzed. Submerged cell results, the first approach used in the development of eU2A device, will focus mostly on the main problems encountered for this reaction to occur. Different membranes and catalysts were used, but due to the overload of parameters that could be changed, a new route was taken. The rotating disk electrode method helps to understand the behavior of certain electrocatalysts without having to take the mass transport factor into account (gas bubbles should detach quickly). With this method, the most suitable catalyst was chosen to proceed with measurements in a third device. Continuous closed cells have the advantage of forced convection of reactants through the MEA, limiting the mass transport losses again. In this cell, CCM *vs* CCS was studied, with different commercial membranes and components.

Fifth chapter focus on the conclusions drawn from all the work elaborated and the results obtained are presented and compared to the objectives stablished. In the sixth chapter, a self-evaluation of the work done is presented as well as an evaluation of the objectives achieved.

2 Context and State of the art

2.1 Diesel Engines and reduction of emissions

Diesel engines or compression-ignited (CI) engines present great advantages for use in land and sea transport, mostly due to higher efficiencies than spark ignition (SI) (gasoline) engines.

For compression-ignited engines, air in cylinders is already at higher temperatures and pressures than the ignition point of the fuel. It means that when the fuel enters the cylinder, it is consumed right away, and power is produced [8]. For spark ignition engines, this does not occur, a spark is needed to ignite the fuel. One downside of this is engine-knock, phenomena where the fuel self-ignites after increase in temperature and, over time, originating engine failures [9], leading to lower efficiency when compared to compression-ignited engines. However, compression-ignited engines also have their flaws. They normally operate with excess air, which, with the high temperatures of operation, causes particulate matter (PM), CO, hydrocarbon (HC) and nitrogen oxides (NO_x) to form and be emitted out of the tailpipe. In compression-ignited engines, thermal NO_x (Zeldovich mechanism) formation is the most predominant mechanism, consisting of oxidation of N_2 from atmospheric air at a high-temperature [10-12]. From this reaction, mainly nitric monoxide, NO, is produced. Later, at lower temperatures, NO can be reduced into nitrogen dioxide, NO_2. Other NO_x species can be found in negligible amounts[13]. NOx is produced mainly from two reactions, as follows:

$$N_2 + O_2 \rightarrow 2NO \tag{2.1}$$

$$NO + ½O_2 \rightarrow NO_2 \tag{2.2}$$

Mitigating emissions from these pollutants is of the upmost importance, with governments and legislators, especially in Europe, getting increasingly strict in the regulations for automotive and industry emissions (Euro V and VI regulation for cars) [4]. Reduction of CO and hydrocarbons can be achieved effectively using diesel oxidation catalysts (DOCs) and particulate matter is removed with diesel particulate filters (DPFs). NO_x emissions on the other hand, are still harder to control and reduce. Selective Catalytic Reduction (SCR) is the main technology for automotive and industrial applications when it comes to “DeNoxing” due to its low cost and high removal efficiencies [13]. Fig. 2.1 shows mainly mechanism for exhaust gas aftertreatment for the majority of diesel cars.

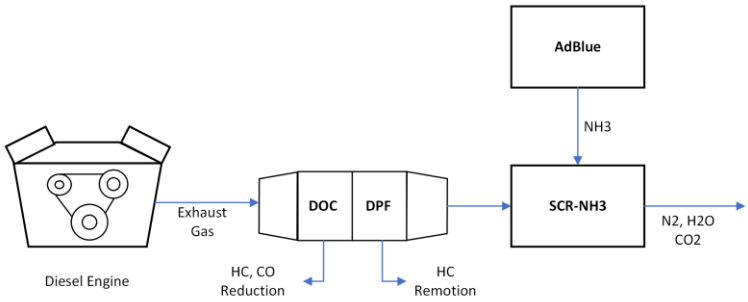

Figure 2.1-Representation of exhaust-gas after treatment in a diesel car- adapted [14, 15].

2.1.1 Ammonia-Selective Catalytic Reaction

Current catalysts used in industrial and automotive applications for SCR, V_2O_5 -WO_3 (MoO_3)/TiO_2, for example [16], perform badly at temperatures below 300 °C [17]. It is then evident that SCR has some limitations [17], since exhaust gas temperatures in cars have diminished over time because of exhaust gas recirculation use [18]. There is also one more constraint that influences SCR reliability, connected to the fact that diesel cars, prevalent in Europe, must be prepared to work even when atmospheric temperatures are lower during colder months and when cars have cold-starts [19].

The typical stoichiometric reactions in SCR, using Vanadium Oxide-based catalysts, are the following (equations 2.3-2.4) [13].

$$4NH_3 + 4NO + O_2 \rightarrow 4N_2 + 6H_2O \quad (2.3)$$

$$4NH_3 + 2NO_2 + O_2 \rightarrow 3N_2 + 6H_2O \quad (2.4)$$

2.1.2 Urea to ammonia conversion

Thermal Hydrolysis of Urea

SCR reaction has ammonia as one of its reactants for NOx reduction. Due to the toxicity of ammonia, urea ($CO(NH_2)_2$) is used in its place (Figure 1), for mobile applications, functioning as an ammonia storage agent. This is normally done by exposing diesel exhaust fluid (DEF), also known as AdBlue, to high temperatures, leading to water evaporation first and then thermal hydrolysis of urea (THU). This reaction forms ammonia and isocyanic acid, which itself will hydrolyze into ammonia and CO_2 [16]. These reactions can be better understood below (equations 2.5-2.7):

$$CO(NH_2)_2 \cdot xH_2O \rightarrow CO(NH_2)_{2(s)} + xH_2O_{(g)} \quad (2.5)$$

$$CO(NH_2)_{2(s)} \rightarrow NH_{3(g)} + HNCO_{(g)} \quad (2.6)$$

$$HNCO_{(g)} + H_2O_{(g)} \rightarrow NH_{3(g)} + CO_{2(g)} \quad (2.7)$$

Thermal hydrolysis of urea efficiency, like NOx reduction by ammonia, is very dependent on high temperatures. For these reactions, temperatures below 280 °C start to be problematic and at 200 °C it is very difficult for urea to ammonia conversion (U2A) to happen [15]. A great amount of research has been done with different catalysts and technologies based around SCR, to achieve better performances in colder conditions, maintaining great conversion efficiencies [20]. Nevertheless, most up-and-coming technologies still need to operate at high temperatures and use electrical heaters to raise exhaust temperature at cold start.

Electrochemical urea to ammonia (eU2A)

An emerging possibility for U2A conversion is the use of low temperature electrolytic cells in alkaline media, either alkaline or anion exchange membrane electrolysis, for electrochemical conversion of urea into ammonia (eU2A) and hydrogen (Fig.2.2) [21]. These electolytic technologies, explored with further detail in chapter 2.2, are subject to a lot of R&D for normal water electrolysis, with alkaline technology being more mature and AEM a more recent and promising option for green hydrogen production.

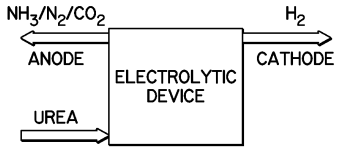

Figure 2.2- Electrolytic cell for production of ammonia and hydrogen, extracted from [21].

For this eU2A, Ni-based catalysts seem to be the most actives. Urea decomposition at NiOOH was firstly studied by Darmola *et al.* in 2010 [22]. They based their research on a natural enzyme urease and tried to replicate its behaviour with the aforementioned catalyst. NiOOH is the product of Ni catalyst oxidation in alkaline media (equation 2.8). Using density functional theory (DFT), the author also proposed reaction mechanism for dissociation of urea at NiOOH (equations 2.9-2.11):

$$\cdot\mathrm{Ni(OH)_2} + \mathrm{OH^-} \rightarrow \mathrm{NiOOH} + \mathrm{H_2O} + \mathrm{e^-} \tag{2.8}$$

$$\mathrm{CO(NH_2)_2} + \mathrm{NiOOH \bullet OH^-} \rightarrow [\mathrm{NHCONH_2 \bullet Ni(OH)_2OH}]^-_{\mathrm{ads}} \tag{2.9}$$

$$[\mathrm{NHCONH_2 \bullet Ni(OH)_2OH}]^-_{\mathrm{ads}} \rightarrow [\mathrm{NCO \bullet Ni(OH)_2OH}]^-_{\mathrm{ads}} + \mathrm{NH_3} \tag{2.10}$$

$$[\mathrm{HNCO \bullet NiOOH}]_{\mathrm{ads}} \rightarrow \mathrm{NCO^-} + \mathrm{NiOOH} \tag{2.11}$$

In NIOOH, as in urease, Ni atoms and a hydroxide group function as active sites for urea dissociation [23]. Ni atoms are predicted to interact with N and O atoms in urea and hydroxide group will interact with the C atoms. Using density functional theory, Daramola *et al.* [22] predicted mechanisms and products of complete urea dissociation into ammonia and carbon

dioxide at NiOOH catalyst. They also predicted the kinetics for different reaction mechanisms for the complete Urea Electrooxidation reaction proposed and their steps.

The eU2A from AdBlue is not only a great low-temperature alternative to thermal hydrolysis of urea (THU), but also gives an opportunity for on-board production of H_2, which, as mentioned before, can be used as a reducing agent of NOx (H2-deNOX) at lower temperatures than ammonia. This will mean increasing conversion efficiencies for a wider range of temperatures [24].

With eU2A, ammonia production can be decoupled from the exhaust system Fig. 2.3 leading to better urea conversion and, with that, better DeNOx efficiency. Botte *et al*. Presented for the first time this technology, obtaining 28 times the rate of ammonia generation in 24 hours, when compared to thermal hydrolysis of urea, at 70 °C. Furthermore, the estimated rate constant for eU2A at 70 °C was 30 % higher than the rate constant found in the literature for THU at 140 °C [25].

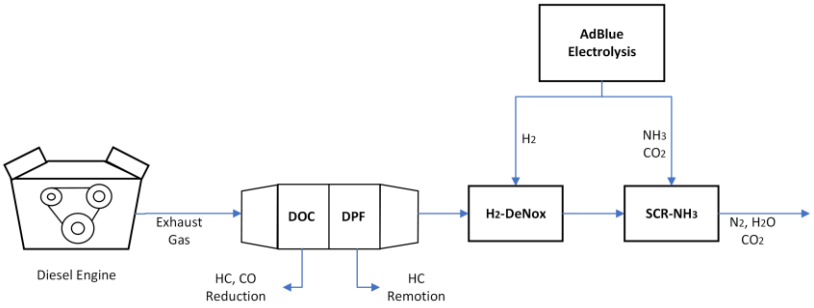

Figure 2.3- Exhaust gas treatment with H_2-DeNOx treatment and decoupled Urea decomposition.

Besides Ni-based catalyst, little is known about other catalysts for this reaction for both anode and cathode. Admitting that conditions on the cathode are no different from normal water electrolysis, conventional cathodic catalysts for AWE and AEMWE can be used. For the anode, a balance between what are the state-of-the-art catalysts for AEMWE and urea-assisted water electrolysis should be achieved. In this case, neither urea should be oxidized completely, nor OER should be dominant, poisoning the sites for urea hydrolysis.

2.1.3 Hydrogen deNOx (H2-deNOx)

NO_x reduction by H_2 has gained attention as a promising alternative/complementary approach to ammonia and urea SCR, mainly due to high efficiencies at low temperatures, ideal for city driving, cold starts, and stop-and-go traffic where normal SCR lacks efficiency. H_2-deNOX (equation 2.12) is very similar to ammonia NO_x reduction (equation 2.13), presenting some drawbacks that are not considered in normal SCR technology like the use of precious metal catalysts like Platinum and Palladium [26] and 2 competitive reactions (equations 2.13-2.14), the first one will produce N_2O, a greenhouse gas, and the second one will consume H_2,

thus influencing conversion efficiency. However, it also can tolerate sulphur content in the exhaust gas more easily [24].

$$2NO + 2H_2 \rightarrow N_2 + 2H_2O \quad (2.12)$$

$$2NO + 2H_2 \rightarrow N_2O + H_2O \quad (2.13)$$

$$O_2 + 2H_2 \rightarrow 2H_2O \quad (2.14)$$

Kureti *et al.* [27] demonstrated that high NO_x conversions (90 %) can be achieved at temperatures between 130 °C and 215 °C, while having great N_2 selectivity, minimizing N_2O production.

2.2 Anion Exchange Membrane Water Electrolysis

Anion exchange membrane water electrolysis (AEMWE), despite its novelty, is quite promising and with a lot of research being currently done around it. In the last few years there was a noticeable increase in number of publications on this topic. Only in the last decade publications rose from 10 in 2012 to 146 in 2022 [28].

Working principle for AEMWE is the same as most other electrolysis technologies. However, in this case, OH^- ion is exchanged through a nonporous polymer membrane commonly called Anion-Exchange Membrane (AEM). Reaction is the same as AWE and occurs as follows (equations 2.15-2.17) [29]:

$$\text{Anode: } 2OH^- \rightarrow \frac{1}{2}O_2 + H_2O + 2e^- \quad E° = 0.40\ \text{V}\ vs\ \text{RHE} \quad (2.15)$$

$$\text{Cathode: } 2H_2O + 2e^- \rightarrow H_2 + 2OH^- \quad E° = 0.83\ \text{V}\ vs\ \text{RHE} \quad (2.16)$$

$$\text{Net reaction: } H_2O \rightarrow H_2 + \frac{1}{2}O_2 \quad E^{\circ}_{rev} = -1.23\ \text{V} \quad (2.17)$$

AEMWE technology has the advantage of a zero-gap setup, where an AEM works as a solid electrolyte for ion conduction while serving as an electron barrier and is used to separate anode and cathode without a liquid electrolyte in between [29, 30]. This compares to PEM electrolyzers setup and enables higher operating pressures for the cathode, higher current densities (due to lower internal losses), and higher gas purity. However, to increase performance, AEMWE still uses KOH in water as a supporting electrolyte to promote OH^- conductivity The use of a diaphragm/separator in AWE prompts gas crossover and higher ionic resistance. In AWE, these parameters are related to the distance between electrodes and the separator. If the distance increases, there will be a lower gas crossover (higher purity), but it will compromise ionic resistance (lower current density), and vice versa. Because of the zero-gap feature, AEMWE and PEMWE are both more efficient and safer technologies than AWE, with

AEMWE using lower KOH concentrations. Safety comes from high purity mostly, since gas crossover can create safety problems from H_2 and O_2 mixture, which can be explosive.

AEMWE also mimics AWE by using transition-metal catalysts instead of the rarer and more expensive Platinum Group Metals (PGM) used in PEMWE. It also enables the use of stainless steel (SS) or nickel components (bipolar plates and porous transport layers) rather than titanium ones. A brief SWOT analysis (strengths, weaknesses, opportunities, and threats) is presented below, based on Guilbert *et al.*, who have done the same assessment for AWE and PEMWE [30-32].

Table 2.1-SWOT analysis on AEMWE-based on Gambou et al. and Zakaria et al. [30, 31].

Strengths	Weaknesses
• Zero-gap cell design • Low-cost cell materials • Non-Noble metal catalyst • High operating pressure	• Still at early stages (TRL 4-6)[33] • Low durability • Membrane degradation • Excessive catalyst loading • Low current densities
Opportuinities	**Threats**
• Development of highly stable and reliable AEMs • Critical status of PGM • Need for cheaper stackable WE technology	• Development of better catalyst for PEMWE • Decrease of PEMWEs capital cost • Lack of substitutes for cathode catalyst (Pt/C)

2.2.1 Anion Exchange Membrane

AEM can be identified as the main obstacle for the lack AEMWE large-scale deployment, at least in the near future. Despite being potentially cheaper than Nafion-Based membranes [30] and having a lot of research being done on it, AEM still lacks ionic conductivity and low chemical and mechanical stability. This will lead to bad performances in long term operation, which is a dissuasive factor for real life applications. As a result, research in AEMWE is very focused on new stable membranes, adequate for high-pH and high-temperature operation conditions, with greater OH^- conductivity, closer to that of a Nafion-Based membranes (comparable to H^+ conductivity) [34].

AEM consists of polymeric backbones with cationic head groups attached. These head group's main function is conductivity and selection of OH^- ions (preventing gas and water crossover). Several types of cations can be used in AEMs, affecting chemical stability and ion conductivity [35]. Main cation groups used are nitrogen-based groups, such as quaternary ammonium (QA) ions. These ions are easy to synthesize and have good ionic conductivity while having a good stability when compared to other cation groups. However, there are some

problems linked to ammonium group attack by OH^- ion and nucleophile substitution. Other cation groups used are imidazolium cations, phosphonium cations and very promising organometal cations [34]. For cation group incorporation, there is the possibility of direct polymerization or post-polymerization and functionalization of the groups in a pre-formed backbone [36].

Regarding backbones, poly(arylene ether)-based, polyolefin-based (such as polystyrene and polyethylene), polyphenylene-based and polysulphone-based backbones are mainly used due to their known relative alkaline stability. These polymers must ensure mechanical and thermal stability to the membrane [34].

For performance evaluation of AEMs, conductivity, ion exchange capacity (IEC), water uptake (WU) and swelling ratio are normally the main indicators. Hydroxide conductivity is considered the parameter with the greatest influence in membrane performance. This can be improved by increasing cation group content (IEC). However, there is also a balance that has to be met. High ion exchange capacity , beyond a certain point, leads to excessive water uptake and high swelling ratios [37], with both phenomena being related to decreased mechanical stability of the membrane. Attached to this work, there is a table presenting some properties and prices for commercial membranes available, some of them being used during this work. Anion exchange ionomers (AEI), which will be mentioned later, are normally coupled with the corresponding membrane and so, membrane optimization and choice should always take into consideration the pair.

2.2.2 Hydrogen Evolution Reaction and Oxygen Evolution Reaction catalysts

HER and OER are heterogeneous reactions, where electrons are transferred to and from the reactants, throughout an electrode, with the presence of liquid reactants and gaseous products. Catalyst optimization focus mainly on using low cost and non-rare materials for this technology, mostly on the anode side. However, these materials come with their downsides, namely the lack of knowledge and lack of stability of these potential catalysts. Electrocatalyst development focus on achieving both high activity and stability. Good activity can be achieved either by increasing the number of active sites or by increasing the intrinsic activity of the catalyst for the reaction [38]. More active electrocatalysts will display lower overpotentials (η), which means that voltage between theoretical potential and effective potential needed for the reaction to occur is lower. Electrocatalysts must have good activity as a powder along with a similar good behaviour in the catalyst layer for the device in real operation conditions. In terms of stability, the most used metric is the S-number, a ratio between the amount of product (either O_2 and H_2) and the amount of dissolved catalyst. This can be used to find a balance between the activity of the catalyst and its degradation. Most prevalent factors responsible for catalyst deactivation and degradation are surface poisoning from side or unwanted reactions,

detachment from the support or the coated surface, metal dissolution and morphological and/or compositional changes [29, 39, 40].

HER

Generation of hydrogen has been well documented, and it is stablished that three consecutive steps take place: Volmer, Heyrovsky and Tafel. The three steps are presented below, for alkaline media, with * representing adsorbed species in the active sites of catalyst (equations 2.18-2.20) [29, 36, 41].

Volmer: $$H_2O + e^- \rightarrow H^* + OH^- \quad (2.18)$$

Heyrovsky: $$H_2O + H^* + e^- \rightarrow H_2 + OH^- \quad (2.19)$$

Tafel: $$2H^* \rightarrow H_2 \quad (2.20)$$

HER kinetics are known as being sluggish in alkaline medium and much slower than in acidic electrolyte, due to the lack of protons for the Volmer step, where hydrogen adsorbs in the active site [42].

In terms of catalysts, and despite being a noble metal catalyst, Pt/C is widely used, even in alkaline media, with great results. An optimum catalyst should present a near 0 value for Gibbs free energy of hydrogen adsorption (ΔG_H). Negative values will mean great activity not only for reactants but also for products and intermediate species, resulting in the poisoning of the catalyst. Positive values reveal a lack of activity for the reactions to take place. Pt/C presents a near zero ΔG_H, thus being the almost uncontested catalyst for HER, as mentioned previously. Some research is being done for PGM-free catalysts aiming to increase the sustainability and viability of large-scale hydrogen production, with Ni being the main element used for these catalysts. By itself, Ni nanopowder shows poor performance as the catalyst for the cathodic reaction in AEM [43]. However, when alloyed with other metals such as Mo, Co, Cu, Ce, Fe, and Al, performances close to those of Pt/C were achieved. Nonetheless, concerns over stability and the actual electrochemical surface area of the catalysts (ECSA) still limit their use. Combinations of Pt with Ni also increase catalyst activity in alkaline media [44]. This synergy can be done either by alloying both metals or by Ni/NiFe cluster deposition in Pt [45, 46]. Ni-Mo alloys are also quite promising, either as binary (both elements only) or trinary alloys (Ni-Mo with some of the transition metals above) [47, 48]. Zhai *et al*. [49] also presented an electrocatalyst, NiSe, resulting from $NiSe_2$ phase transformation and it showed improved results for HER reaction in alkaline medium.

OER

Oxygen evolution reaction (OER) in alkaline medium occurs in a four-step pathway with OH^- as an intermediary and the transference of four electrons instead of the two from HER (equations 2.21-2.24) [36, 41].

$$4OH^- \rightarrow 3OH^- + e^- + OH^* \quad (2.21)$$

$$OH^* + 3OH^- + e^- \rightarrow 2OH^- + e^- + O^* + H_2O \quad (2.22)$$

$$O^* + H_2O + 2OH^- + 2e^- \rightarrow OH^- + 3e^- + OOH^* + H_2O \quad (2.23)$$

$$OOH^* + H_2O + OH^- + 3e^- \rightarrow 4e^- + OOH^* + 2H_2O + O_2 \quad (2.24)$$

Even with some problems for HER in an alkaline medium, OER still has the worst reaction kinetics. Thus, OER is the controlling reaction for the electrochemical system's efficiency and energy use.

In PEMWE, state-of-the art catalyst and PGM IrO_2 and RuO_2 are used in the anodic reaction. This is due to the low pH in addition to high voltages of OER, region where only PGM based catalysts can operate without corroding [29]. On the other hand, for OER in alkaline media, there is the appealing advantage of being able to use non-PGM catalysts. In the case of AEMWE, metal oxides and (oxy)hydroxides catalysts based on transition metals like Ni, Co, Fe and Cu can possible be used as alternatives to IrO_2 and RuO_2. In AWE, these types of catalyst are already used in anode electrodes for commercialized solutions. Despite this, OER's high pH and voltages in AEMWE limits the use of catalysts with carbon supports, that are widely used in HER, with good results. In these harsh conditions the carbon support would be quickly and easily oxidized, losing is functionality [29].

From all the transition metals mentioned above, Ni-based catalysts are, once again, the most promising ones, even if coupled with some other elements. These catalysts are mostly unsupported, high-surface-area alloys such as Ni_xFe_y and $Ni_xCo_zFe_y$ [29]. It is commonly understood that these alloys, when exposed to voltages below the onset of the OER, around 1.3-1.4 V *vs* RHE and in alkaline media, will oxidize forming oxides and/or (oxy)hydroxides (eq. 2.11) [50, 51]. These species are much more active OER catalysts than their non-oxidize counterparts, in alkaline media [52]. There is still some uncertainty about Ni_xFe_yOOH. Several studies point out that despite being the most active catalyst in a three-electrode cell (RDE), they have the worst performances in AEMWE due to poor conductivity and low stability between ionomer and catalyst particles [52, 53]. There is also some uncertainty about the real active sites and what is the optimum proportion of Ni/Fe. Anatharaj *et al*. report the main roles of Fe and its ions. They suggested that Fe^{3+} increases conductivity and it is an active site for intermediate steps in OER, but it also helps the oxidation of Ni^{3+} into Ni^{4+}, a highly active specie that facilitates intramolecular oxygen coupling [54, 55].

Besides particle-based catalysts, there is also the possibility to incorporate catalysts in porous supports. NiFe-layered double hydroxides (NiFe-LDH) are a big example of that. These are low-cost materials made of ultrathin nanosheets (even single atoms thickness) with similar structure of $Ni(OH)_2$, compound that will later result in highly active NiOOH as previously

mentioned. LDH catalyst are normally incorporated into porous conductive substrates such as Ni foam/felt or carbon nanotubes [56, 57].

2.2.3 Membrane Electrode Assembly

The association of the membrane and the anode/cathode catalyst layer is commonly known as membrane electrode assembly (MEA). This is the central piece in a water electrolyzer with zero-gap setup. In there, an equilibrium between liquid reactants, gas products, electrons and ions must be achieved.

MEAs are divided in 3 groups, depending on the surface where the catalyst layer is coated: catalyst-coated membrane (CCM), catalyst-coated substrate (CCS) or the combination of both methods, one for each electrode (CCM-CCS). In the CCM case, catalyst is directly deposited on the polymeric membrane (AEM). For CCSs, catalyst is deposited on the porous transport layer (PTL) or in porous substrate that will stay between the membrane and the bipolar plates. CCM offers several advantages over CCS, and it is considered the end goal setup.

One variable extremely important for good MEA performance is the catalyst layer. Catalyst layer optimization focus on achieving the best possible pathways for all the species involved in the reaction. High-density of reaction points within the triple-phase boundary is pivotal for good MEA performance. The triple phase boundary can be described as the area in the catalyst where the liquid reactant (water), electrolyte (OH^-), the solid (catalyst particles) and the products (O_2 or H_2) all coexist, being ideal for the reaction to occur [55].

Catalyst layer is normally deposited using an ink or slurry that is then sprayed or printed in the desired surface. Spray coating is the most conventional technique in AEMWE and resorts to the use of an automated ultrasonic spray-coating machine allowing low flow rates of ink to be coated on surface that is being heated at 60 - 80 °C. This will make the solvents evaporate quickly and prevent membrane swelling or absorption by the substrate. Despite the possibility of flooding and thermal degradation of the membrane in spray coating, ink preparation is easier, and rheology is less relevant than in printing methods. Other deposition methods range from film casting, offset printing, screen printing and blade coating. Printing methods like these can be more feasible for large-scale and continuous manufacturing. Less used possible techniques, with thin-film deposition like vapor deposition, atomic layer deposition and others are being investigated to decrease the amount of waste and solvents used.

For ink preparation, besides the catalyst, solvents and an anion exchange ionomer (AEI) are used. The normal mixture of solvents used is usually a mixture of isopropanol and ultra-pure water. The ionomer used should preferably be chemically identical to the membrane used (same cation/backbone) to avoid/decrease interfacial resistance. AEI functions as an ionic bridge between the membrane and the catalyst layer and can also be used as a particle binder

[29]. The amount of ionomer used is normally a function of the solids in the catalyst ink and should be enough to promote good ionic conductivity in the MEA. However, an excessive amount can increase electronic resistance, will block active sites, decrease porosity, and with that increasing mass transport resistance, and it can also lead to particle detachment due to overhydration from excessive water uptake [58, 59]. AEI mass percentage is the weight of ionomer per total mass of solids in the ink and normally differs for anode and cathode. For the anode, values around 7 – 15 wt% [53, 60] of the total solids are commonly used, but it can go as low as 4.5 wt% [61] and up to 25-30 wt% [62]. On the cathode side, percentages between 10 - 40 wt% can be used without real difference in the performance [63, 64]. Most of the time, the pair catalyst-ionomer should be studied individually to find the best AEI content for each situation. AEIs with high ion exchange capacity values would theoretically allow better performances, but it can lead to an increase in water uptake (WU), which has been demonstrated to have a great influence on MEA performance [62]. Most commercially available AEIs are still very unstable at high temperatures in the long term, mainly at high pH. Due to their binding effect, when degraded, AEIs will detach from the catalyst layer and will lead to catalyst deactivation and degradation. On top of that, the oxidation of AEIs containing phenyl groups can lead to a local decrease in pH and possible catalyst poisoning [29].

CCS in alkaline media must be well thought through because of stability issues. The substrate used has not only to be a good conductor between the porous transport layer (PTL) or the bipolar plates (BPP) and catalyst but also as mechanical support to the membrane. Contact between ionomer in the catalyst layer and the membrane is more difficult for CCS and so, ion conductivity will be lower in the MEA. For the cathode side, mostly carbon paper and carbon cloths are used as substrates, but there is also the possibility of using Ni and Ti materials. For the anode, and because of the harsh alkaline conditions with high voltages, carbon materials can't be used. Ni foams/felts and Ti material are used. Stainless steel (SS) substrates are less desirable because in alkaline media and high voltage, SS passivates, causing higher electronic resistance [65].

CCM provides a closer contact between catalytic layers and membrane and thus improves the conductivity of OH^-. However, there is the worst contact between the catalyst and current collectors/PTLs. This can induce higher resistance in the system. Nevertheless, CCM presents itself as the best approach, since OH^- conduction is much more limiting and difficult than electronic one. Spray coating is normally the best coating technique since other methods used in PEMWE, like decals, have a hot-pressing step that can degrade the membrane [66]. Despite presenting itself as the best theoretical solution, there are still some concerns about MEA stability when manufactured by CCM, mainly due to membrane drying and ionomer degradation. Up to the time of writing, the results of CCM *vs.* CCS are very close, with no clear winner. This

can also be related to lack of standard testing protocol. Mixed MEAs, CCM-CCS, can be a solution for ionomer and catalyst degradation on anode side. With that, CCM would be done on the cathode side, while CCS method could be created on the anode side, even possibly using incorporated catalysts in a porous substrate (already mentioned in the OER subchapter)

One last important parameter is torque used for MEA's compression. In PEMWE, MEAs are normally hot-pressed before cell assembly for better catalyst adhesion. In AEMWE hot pressing or just pressing the membrane is a very delicate matter. While higher compression will always lead to better performances because it decreases interface and ohmic resistances, AEMs tend to be much thinner than membranes used for PEMWE and so, compressing them between substrates or PTLs may originate punctures and damages that can cause short-circuits [67]. Normal torques for MEA's compression in AEMWE, depending on the MEA constituents and the setup, range from 2-6 N·m [67, 68].

2.2.4 Operating Conditions and other components

Operating conditions and other components such as bipolar plates (BPP) and gaskets have some importance for good AEMWE performance. BPPs for AEMWE are mainly made off Ni and SS materials, which decreases a lot the price compared to PEMWE, where Ti BPPs are normally used. They can have flow channels to increase distribution of water across the PTL and consequently the MEA. Nonetheless, carving flow fields will increase significantly the cost for these materials. There is the possibility not using flow field [69] but this could influence distribution of the reactants. Goal for BPP optimization in AEMWE is the use of mainly SS materials without compromising long term stability but more studies in this area are needed since a lot of research is still being done with the same Ti BPPs used in PEMWE.

Optimum **temperature** of operation is essential for overall cell stability and more specifically, as mentioned before, AEM and AEI stability. Above 60 °C, MEA degradation, for most membranes, is expected [29]. Increasing temperature of operation to around 80 °C, similar to PEMWE [66], is then a priority in order to decrease cell potential (E_{cell}) and with that improve performance (increasing current density) [29].

Supporting/feeding electrolyte is normally needed to help OH^- conductivity and with that have better performances than just pure water feeding. Razmjooei *et al.* [70] studied the effect of KOH concentration in an AEMWE cell. They studied several concentrations between 0.1 - 1 M KOH and concluded that great increases in performance happen when it goes from 0.1 M to 0.3 M. However, no substantial improvements are seen from 0.3 M to 0.5 M and finally to 1 M due to excessive gas bubbling and high viscosity. This suggests that 0.3 M could be a good ion exchange capacity optimum value. Nevertheless, every setup should be studied individually, mostly depending on AEMs and AEIs that can coupe or not with the lack of electrolyte or with the excess of it, depending on ion exchange capacity.

High operating **pressure** is one of the advantages of AEMWE and PEMWE over AWE. Differential pressure between cathode and anode (pressurized cathode) increases H_2 purity as oxygen crossover is lowered. Moreover, H_2 gas product already around 30 bar will facilitate its storage and can prevent the use of upstream pressurizer. Nonetheless, high pressure at the cathode can also lead to hydrogen crossover. This creates two main problems; besides losing the product wanted, it can also create a dangerous mixture (explosive) of O_2 and H_2 [71]. Other possible problem is membrane mechanical stability leading to thicker membranes use, decreasing performance.

Finally, for continuous flow closed cells, flow optimization has some importance to prevent the membrane's drought. Cathode side doesn't need water during operation, leaving it dry could even be beneficial [72]. On the other hand, anode side feed flow rate should be optimized in each situation, but typical values for this range from 1-10 $mL \cdot cm^{-2} \cdot min^{-1}$, which amounts for 4 - 40 $mL \cdot cm^{-2} \cdot min^{-1}$ in stacks/cells with 4 cm^2 MEAs. Flow rate needs to be high enough to prevent mass transport limitations and scarcity of reactants.

2.3 Urea-assisted Water electrolysis

Different than electrochemical conversion of urea to ammonia but with close similarities, urea-assisted water electrolysis (UWE) intends to couple the electrochemical production of hydrogen from water with complete urea oxidation reaction (UOR) (equation 2.25). This originates H_2 as one of the reaction products.

$$CO(NH_2)_{2(aq)} + H_2O_{(l)} \rightarrow N_{2(g)} + 3H_{2(g)} + CO_{2(g)} \quad (2.25)$$

For this work, despite the interest in oxidation of urea until ammonia production,further urea oxidation until N_2 production is not intended. Nevertheless, some mechanisms are similar and because this topic has a lot more research done or being done on than eU2A, some procedures, operating conditions and materials can be based on this technology. Firstly, described by Botte *et al.* in 2009 [73], a novel technology where electrolysis of urea from urine for hydrogen production was suggested. They studied the use of Ni catalysts in an Alkaline electrolytic cell. Articles with research of alkaline water electrolysis assisted by urea decomposition/oxidation followed. Some works propose complete oxidation of urea into N_2, others, much scarce and already mentioned, suggest oxidation of urea just until ammonia production. No articles on AEM water-urea assisted electrolysis has been published at the time of writing, at least of the author's best knowledge.

3 Materials and Methods

In this chapter, three different testing methodologies are going to be explored: submerged cells, rotating disk electrode (RDE) and a closed electrolyzer cell.

Catalysts take a big part during all three experimental set-ups. Specifications for all the catalysts used are shown in the table 3.1:

Table 3.1- Catalysts used during this work.

Denomination	*Company*	*Composition*	*Particle Size*
OXYGEN-N	CENmat	na	na
Pt/C	Alfa Aesar	40 %Pt; 60 %C black	2.0-3.0 nm (Pt)
Ir Black	Umicore	99.9% Ir	na
NiFe-Aldrich	Sigma-Aldrich	Alloy, Fe/Ni (0.55:0.45), >97%	<100 nm
Ni-NPs	SkySpring	99.7% Ni	40-60 nm
NiFeZn	Sigma-aldrich	>99% Fe_4NiO_4Zn	<100 nm

3.1 Submerged Cells

Submerged cells offer several advantages over normal closed, continuous electrolyzer cells. They are easier to assemble and to start testing, there is no starvation of reactants, and it also guarantees that the membrane stays hydrated and does not wrinkle throughout the experiments. Around the cell, a supporting electrolyte consisting of water or AdBlue with KOH will be present.

The set up can be imagine as a sandwich, with no sealing on the side, made up of 2 (or 4) BPPs, 2 PTLs, and the MEA in between (Fig. 3.1).

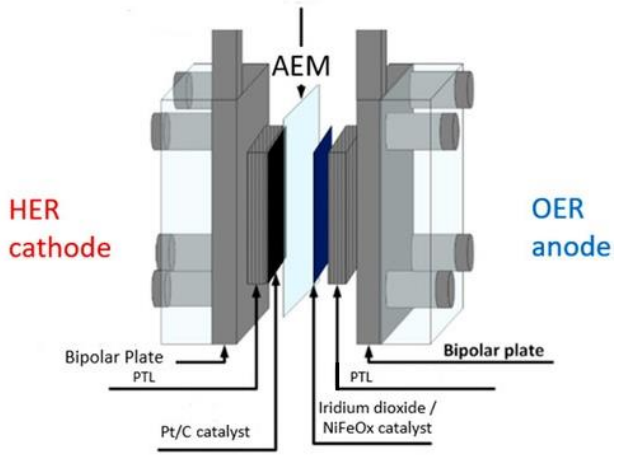

Figure 3.1- Representation of submerged cell setup, taken and adapted from Xu et al. [74].

CCS technique was the exclusively MEA coating technique studied for this setup and both anode and cathode catalyst layers are sprayed into different substrates. Ni felt, Ni foam and 0.23 mm thick 316L SS felt (Bekeart, Bekipor ST 40 type 40 BL3) were used on the anode side,

while graphite paper (0.2 mm thick Spectracarb 1050–2050A) was always used on cathode. BPP used were either SS, Ti or Gold coated and PTLs are mainly SS PTLs from GKN Sinter Metals SIKA-HY with an expanded metal sheet that contacts with BPPs and a macroporous layer that will contact the MEA. In case of urea electrolysis, 2 additional BPPs were used to estimate the BPPs resistance in these electrolytes. BPPs were polished with waterproof sandpaper silicon carbide, with 1000 and 3000 grit from Starcke®. 1000 grit was used all over the plate and 3000 grit was used only to polish the plate surface where the MEA would lie.

Membrane/ionomers used were: Sustanion™ X37-50/XB-7 from Dioxide Materials© PiperION™ A70-HCO3/A-HCO3 from Versogen© and an experimental membrane from a partner company. For all AEMs, a pretreatment was done at least 24 hours before testing, using 1 M KOH solution. This intends to replace ions such as Cl^-/Br^-, used to ensure longevity and functionality of the membranes while stored.

Catalyst inks for spraying were a mixture of the desired catalyst, ionomer, isopropanol, (IPA, C_3H_8O, >99.5% from ThermoFischer Scientific) and ultra-pure water (UPW, Milli-Q 18.2 $M\Omega \cdot cm^{-1}$). After combining all the compounds, the ink was dispersed in an ultrasonic bath (Bandelin Sonocool SC255) at 100% power for 1 h at 20 °C, before spraying. Subsequently, catalyst deposition into the substrate is done using a generic spray gun with a 0.5 mm nozzle using compressed nitrogen at 2 bar over-pressure. During spraying, substrates were positioned with vacuum over a hot plate set to 60 °C, to prevent substrate flooding by evaporating the solvent used in the ink. 1 to 2 hours before assembling the cell, substrates are submerged in 1 M KOH solution for ionomer activation, similarly to membranes' activation. Table 3.2 presents all the essential features of each submerged cell tested during this work.

Table 3.2- Cells used during submerged cell testing and their specifications.

cells	Tested Electrolyte	Membrane	Anode			Cathode		
			Substrate	Catalyst	Loading $mg_{cat} \cdot cm^{-2}$	Substrate	catalyst	Loading $mg_{cat} \cdot cm^{-2}$
SC.1	UPW+ (0.1; 0.3; 0.5; 1) M KOH	PiperION™ A70-HCO3	Ni Felt	OXYGEN-N	4.2	Carbon Paper	Pt/C (40/60%)	0.7
SC.2	AdBlue + (0; 0.1) M KOH							
SC.3	UPW+ (0.1; 0.3; 0.5; 1) M KOH	Sustanion™ X37-50	SS felt	Ir Black	2.5	Carbon Paper	Pt/C (40/60%)	1.2
SC.4	AdBlue+(0; 0.1; 0.3) M KOH		Ni Felt	OXYGEN-N	4.2	Carbon Paper	Pt/C (40/60%)	0.7
SC.5	AdBlue	Experimental Membrane	n/a	n/a	n/a	n/a	n/a	n/a
SC.6	AdBlue+(0; 0.1; 0.3; 0.5; 1) M KOH							

Tests were run with UPW or in AdBlue® (32.5 % Urea Concentration from Höfer Chemie GmbH©) with different concentrations (0.1 M, 0.3 M, 0.5 M, 1 M) of KOH (≥85 % KOH, 56.11 g·mol^{-1} from Carl Roth GmbH©) as supporting electrolytes. Pure AdBlue without KOH was also tested. MEAs' active surface was 4 cm^2 and torques of 0.2-0.6 N·m was used. Cell was tested at temperatures of 50 °C, 60 °C and 70 °C in every KOH concentration. For uniform temperature of the electrolyte used, rotation speeds of 500 - 700 rpm were used.

AEM electrolyzer ell characterizations were carried out firstly with an activation procedure consisting of 10 to 30 s steps at 0 V, 1 V, 1.25 V, 1.5 V and 1.75 V and 1.5 min at 2 V with 20 s increase voltage ramps between the last 4 steps. This approach aims to discharge the cell from any capacitance charge present in it. Afterwards, cells were subject to I-V potential controlled cycles between 1 and 2 V, until a constant peak was achieved (equal or lower current peak than the previous one). This will mean that the membrane reached peak performance. Finally, resistance and electrochemical impedance spectroscopy (EIS) measurements were done at different current densities (A·cm^{-2} or mA·cm^{-2}), depending on the cell performance. For AdBlue + KOH, EISs were recorded at 25 mA·cm^{-2} using an amplitude of 2.5 mA·cm^{-2} and for better performance cells, at 100 mA·cm^{-2} with 12.5 mA·cm^{-2} amplitude. For UPW and KOH, currents of 100 mA·cm^{-2}, 400 mA·cm^{-2} and 2000 mA·cm^{-2} were used with amplitudes of 12.5 mA·cm^{-2} and 50 mA·cm^{-2}, respectively. EIS and IV-curves were recorded using a Zahner Zennium X potentiostat coupled with a Zahner PP241 booster.

3.2 Rotating Disk Electrode

Rotating Disk Electrode, RDE, is an instrument that allows the study of catalyst powder activity, without the need to account for mass transport limitations (bubble formed in the catalytic layer quickly detaches due to high rotation speeds). Reproducibility of this technique is quite difficult, and these results should not be considered as absolute values, but only as a good reference for comparison. They will depend on the operator, electrode surface and the interface of the working electrode.

Main components of this experimental setup are the working, reference and counter electrodes (WE, RE, CE, respectively) (Fig. 3.2). CE used was a Platinum CE from ALS Co., Ltd. WE, from the same company, had a 0.3 cm diameter and glassy carbon (GC) surface. RE, in this case a hydrogen reference electrode (RHE), was acquired from Gaskatel (Mini-HydroFlex), as well as its battery. Separately, another RHE was used as control for possible shifts from the main RHE. It is very important to check electrode shift and it is recommended for RHE to be at least 24 h in the electrolyte that will be studied before starting tests. During first experiments, there was a shift in the RE due to lack of awareness and to the need to change batteries which resulted in fruitless measurements and some damages to the WE GC surface. WE utilization

requires some precautions. Glassy carbon (GC) should be free of scratches and oxidation. After use in one experiment, the catalyst layer should be carefully removed with a wet paper and then polished (1-5 min, depending on the surface appearance) in an Alumina polishing pad with 0.05 um polishing alumina suspension (Alied High tech products, inc). The apparatus used was made of the electrodes and a RRDE-3A from ALS Co.,Ltd (Fig 3.2). The potentiostat used was an Autolab PGSTAT204 from Metrohm© and the software used was NOVA 2.1 from the same company.

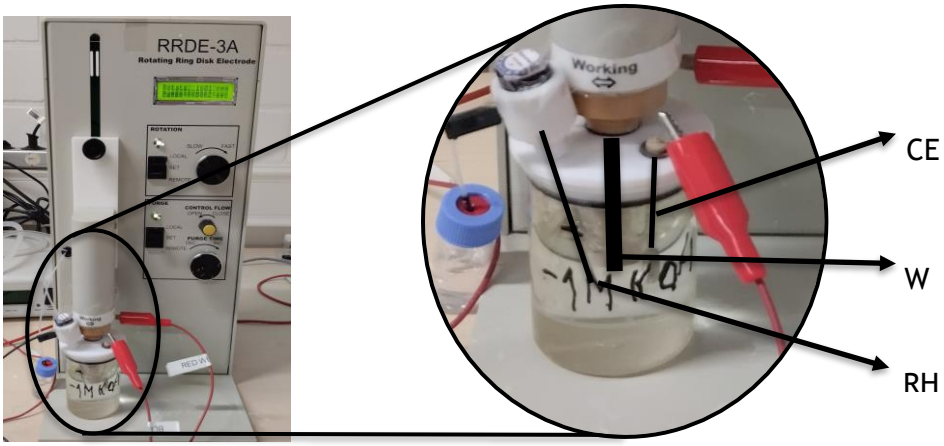

Figure 3.2- Apparatus for RDE experimental tests and closer look into Electrodes used.

For WE preparation, besides polishing, an ink should be prepared, freshly, and then coated on the electrode surface. Ink preparation was firstly optimized to obtain a homogeneous mixed solution. For 10 mg (±1 mg) of catalysts from the table 3.1 was added UPW and IPA in a 3/1 proportion (UPW/IPA), except for "NiFe-Aldrich" where 1/1 was used due to low solubility in water. Because only the anodic reaction was studied, Pt/C was not used in this part of the work The total ink volume stands at 3 mL solution (Fig. 3.3 a)). After brief agitation, Nafion solution (Perfluorinated resin containing 5 wt% Nafion™) was added to obtain an ink with 20 wt% of binder/Ionomer (*ca.* 50 mg). After 15 min of ultrasound bath (Bandelin Sonocool SC255) at 20 °C and 75 - 100 % power, 2.5 µL of solution were taken out and dropped in the electrode surface. The electrode was subsequently dried in an oven, preheated at 50 °C for 2-5 min. These two steps (deposition and drying) were repeated to obtain an electrode with 5 µL solution dropped, which amounts to a 235 $\mu g \cdot cm^{-2}$ loading (Fig. 3.3 b).

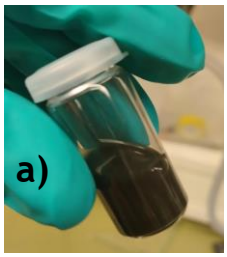

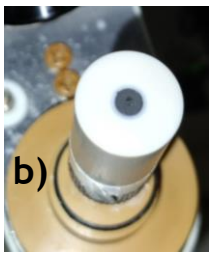

Figure 3.3-a) Example of a catalytic Ink used during RDE experiments, with OXYGEN-N catalyst; b) Coated working electrode with OXYGEN-N catalyst.

During Experiments, different electrolytes were used and they were purged with O_2 and N_2 before and during experiments. Experiments with UPW and 1 M KOH were done as well as experiments with pure AdBlue and AdBlue with 1 M KOH. For UPW and KOH, only N_2 was used to purge, in order to remove CO_2 present in the solution. For the other 2 scenarios, both gases were used to understand if it could have influence in the results. All the tests for RDE were done at atmospheric temperature between 20 °C and 25 °C.

Protocol used for testing included cyclic voltammetry staircases (CV), from 0.4/0.6 V until 1.8 V, at scan rate of 10 $mV \cdot s^{-1}$ and a stability test with four steps at constant potential, for 2 minutes each (1.4 V; 1.6 V; 1.8 V; 2 V). It was concluded that 2V could lead detachment of some catalysts and degradation of the electrode's surface and so, peak potential during CV was reduced to 1.8 V. The number of cycles was 10, by default, but it could be shortened if a steep decrease in performance was noticeable, meaning high degradation.

3.3 Closed Electrolyzer cells

Single closed cell testing is rather similar to submerged cell, in terms of MEA preparation and characterization procedures. Nevertheless, it differs in all other aspects; rather than a support electrolyte, there are feeding solutions going throw flow fields carved in both bipolar plates. This will make the reactants and products move away from the MEA, through forced convection. For this, diaphragm pumps were used (Simdos® 10 from KNF) with different flow rates on the anode and cathode side (this is one of the first parameters that will be studied). Two vessels from where the desired feeding solution was pumped were used for both sides of the cell. During experiments, stipulated to occur at 60 °C, feeding solutions were left at higher temperature due to heat losses through the PTFE tubes. Heating the solution was done using Rotilabo® MH15 from ROTH was used. Despite doing some runs with 0.1 M/1 M KOH in UPW, most tests were done in pure AdBlue and AdBlue with 0.1 M and 1 M KOH. The step-up can be seen in the Fig. 3.4.

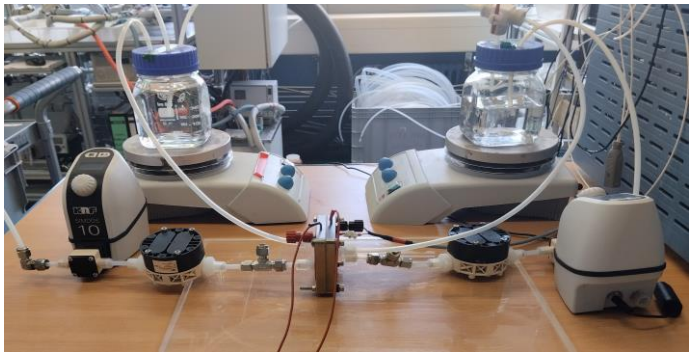

Figure 3.4- Closed Cell test bench with anode on the left and cathode on the right.

The cell itself also has BPPs with heater pads (50 W/110 V from Dioxide Materials™) with a PID controller. During testing, anode's side pad was defective, but temperature of the

cell was still maintained constant. BPPs used for anode and cathode were 5 cm^2 Nickel and 904L SS flow fields, respectively, with serpentine channel, from Dioxide Materials™.

In this set-up, not only CCS MEAs were studied. Mixed MEAs (CCS on the anode/CCM on the cathode) and CCMs were also developed and tested. Here, with the previous knowledge from RDE, only one catalyst was used anode (OXYGEN-N (NiFeOx) from CENmat) and Pt/C from Alfa-Aesar was used on the cathode. All cells used in this experiment are described in the table 3.3. In those cells, different membranes and ionomers were used and thus, comparison between coating techniques cannot be completely straight forward.

Table 3.3- Cells used during testing in closed cell and their specifications.

cells	Tested Electrolyte	Coating technique	Membrane	Anode			Cathode		
				Substrate /GDL	catalyst	Target Loading $mg_{cat} \cdot cm^{-2}$	Substrate	catalyst	Target Loading $mg_{cat} \cdot cm^{-2}$
CC.0	UPW+ 0.1M KOH	CCS	PiperION A70-HCO3	SS felt	Ir Black	4	Carbon Paper	Pt/C (40/60%)	1
CC.1	AdBlue + (0; 0.1; 1M) KOH	CCS	Experimental Membrane	na	Na	na	na	na	na
CC.2	AdBlue + (0; 0.1; 1M) KOH	CCM-CCS	Sustanion X37-50	Ni Felt	OXYGEN -N	4	Carbon Paper	Pt/C (40/60%)	1
CC.3	AdBlue + (0; 0.1; 1M) KOH	CCM	Fumasep FAA-3-50	Ni Felt	OXYGEN -N	4	Carbon Paper	Pt/C (40/60%)	1

During CCMs development, special attention was paid to membrane integrity during spraying. Due to AEMs lack of thermal and mechanical stability, excessive amount of solvent in the ink can lead to severe AEM swelling, greatly compromising MEAs' performance. Moreover, while spraying, it is important to look out for wet spots, where ink accumulation is visible.

To characterize cell, an activation was firstly done, equivalent to submerged cells. After this, potential controlled cycles between 1 V - 2 V were done until constant peak current density was achieved. In these tests, no EIS were done only due to time restraints. Measurements were recorded using a Zahner Zennium X potentiostat coupled with a Zahner PP241 booster when available. When unavailable, QPX750SP power supply from Aim-TTi was used. This equipment was less precise, and its current resolution (10 mA) was unsuitable for these experiments where low current values were obtained.

4 Results and discussion

In this chapter, results of I-V curves are presented always in current density, i ($A \cdot cm^{-2}$ or $mA \cdot cm^{-2}$), rather than direct current measured. This is normal procedure in order to compare different cells from other sources and it is possible to compare between set-ups and experiments more properly.

4.1 Rotating Disk Electrode

Measurements with RDE took the longest out of the three experimental procedures but it was mainly due to inexperience handling the system, ink optimization and damaged or out of order material that had to be replaced. Reference Hydrogen Electrode (RHE) was the main cause of disturbs and unfit results. This subchapter will then be less extensive since most results cannot be considered. Nevertheless, this part of the thesis enabled a better comprehension of RDE operation and the main problems associated with it. The main objective for these measurements was to understand which catalyst could be more suitable for eU2A. Several catalysts were used in UPW+KOH and AdBlue (pure and without KOH) at room temperature. Catalyst used were already mentioned in the Table 3.1.

4.1.1 Ink and deposition Optimization

First step in RDE step was to create good catalytic ink and develop a standard procedure for its manufacturer. This means that the mixture should be homogeneous, and no catalyst particles should be visible. That could be achieved using a good solvent which prevents particle agglomeration. Good ink will result in a better catalytic layer on the surface of the electrode. Fig. 4.1 show the difference between the first catalyst inks (on the left) and the optimized one (on the right). It is visible, in the firs image, that there are almost 2 phases, one with catalyst mixed and another transparent where there is just solvent. Besides that, catalyst particles were visible on the left glass vial. In the second picture, ink was completely uniform.

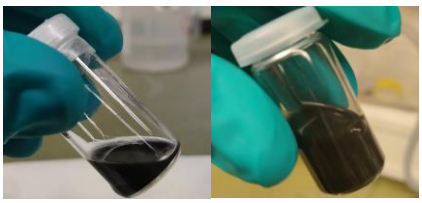

Figure 4.1- OXYGEN-N inks developed for RDE measurement. First ink prepared and optimized one on the left and right, respectively.

The main characteristics looked at were solution volume (increase from 0.2 mL to 3 mL) and ratio between UPW and IPA (it was varied, and the 3/1 UPW/IPA ratio was found to be the

best for most catalysts). However, for NiFe alloy from Sigma-Aldrich, an excesses amount of water was found to be detrimental to ink homogenization and so, 1/1 ratio was used. This analysis was purely qualitative and visual, and no dielectric constants were considered.

Coating optimization was also done. For some time, the presence of a shift in potential for RHE compromised catalyst layer in WE. Very high voltages (above 2.3 V) were achieved which would lead to catalyst and electrode surface oxidation. This meant that catalyst layers would go off the electrode upon the first cycle. However, unaware of this fact, it was thought that poor coating was the reason behind catalyst detachment. After recognizing this problem, proceeding with more experiments and receiving external advice, the optimal coating technique stayed as described in the experimental chapter. As previously mentioned, loading used in these experiments will stay consistent at 235 $\mu g \cdot cm^{-2}$.

4.1.2 Catalyst performance

Figure 4.9 shows how these catalysts behave in UPW with 1 M KOH, pure AdBlue and AdBlue with 1 M KOH. Beforehand, internal resistances of the device with the already coated electrodes were measured for each case. This will allow an eventual correction of the actual potential applied to the electrode surface (U_{cor}), using Eq.4.1, where U is the Potential applied by the working electrode, R is the internal Resistance of the setup that can be measured, and I is the measured current.

$$U_{cor} = U - R\,I \tag{4.1}$$

Fig. 4.2 a) and b) show catalyst performance in pure AdBlue. Catalysts performed very close to each other and were noticeably bad, even factoring in that RDE tests were run at low (atmospheric) temperatures, which has a negative impact on performance. It can also be observed that Ir Black has low stability through the difference between the forward and backward partway of the cycle. In the Ni catalyst run, some “bumps” are noticeable and can be assigned to equipment defects that create noisy responses (some rust in the interior of the working electrode or damaged electrode surface). Overall, performances stayed below 3 $mA \cdot cm^{-2}$. Ni had the best activity, reaching more than 2.5 $mA \cdot cm^{-2}$ while OXYGEN-N performed the worst, reaching 2 $mA \cdot cm^{-2}$

For AdBlue with 1 M KOH, Fig. 4.2 c) and d), OXYGEN-N has performed well above other catalysts, even though in UPW it had approximately the same performance as Ir Black. This demonstrates that Ir is a good catalyst for AEMWE but when urea is present, it is not as active and stable as in pure water. OXYGEN-N peak current density was around 140 $mA \cdot cm^{-2}$, while the second highest performance was achieved by Ni nanoparticles catalyst, with a performance around 50 $mA \cdot cm^{-2}$. It seems safe to consider OXYGEN-N the best performance catalyst in AdBlue, from the choices available. Because there was such a difference between OXYGEN-N and other catalysts, further tests were run with similar results for OXYGEN-N catalyst.

Fig. 4.2 e) and f) displays experiments done in UPW + 1 M KOH demonstrates a clear superiority of OXYGEN-N and Ir Black catalysts. Both these catalysts reached performances around 225 mA·cm^{-2} whereas Ni had a peak current density of 125 mA·cm^{-2}. It can also be seen the Ni^{3+} oxidation into Ni^{4+} has theoretically predicted, for an applied potential of around 1.4 V but this surprisingly not true neither for Ni catalyst nor NiFe-Aldrich, despite redoing experiments to corroborate the results. The reason behind it is not completely clear but could be attributed to catalyst powder or catalyst layer quality. It is also important to mention that OXYGEN-N is already an oxide, and this could facilitate its transformation into oxyhydroxide.

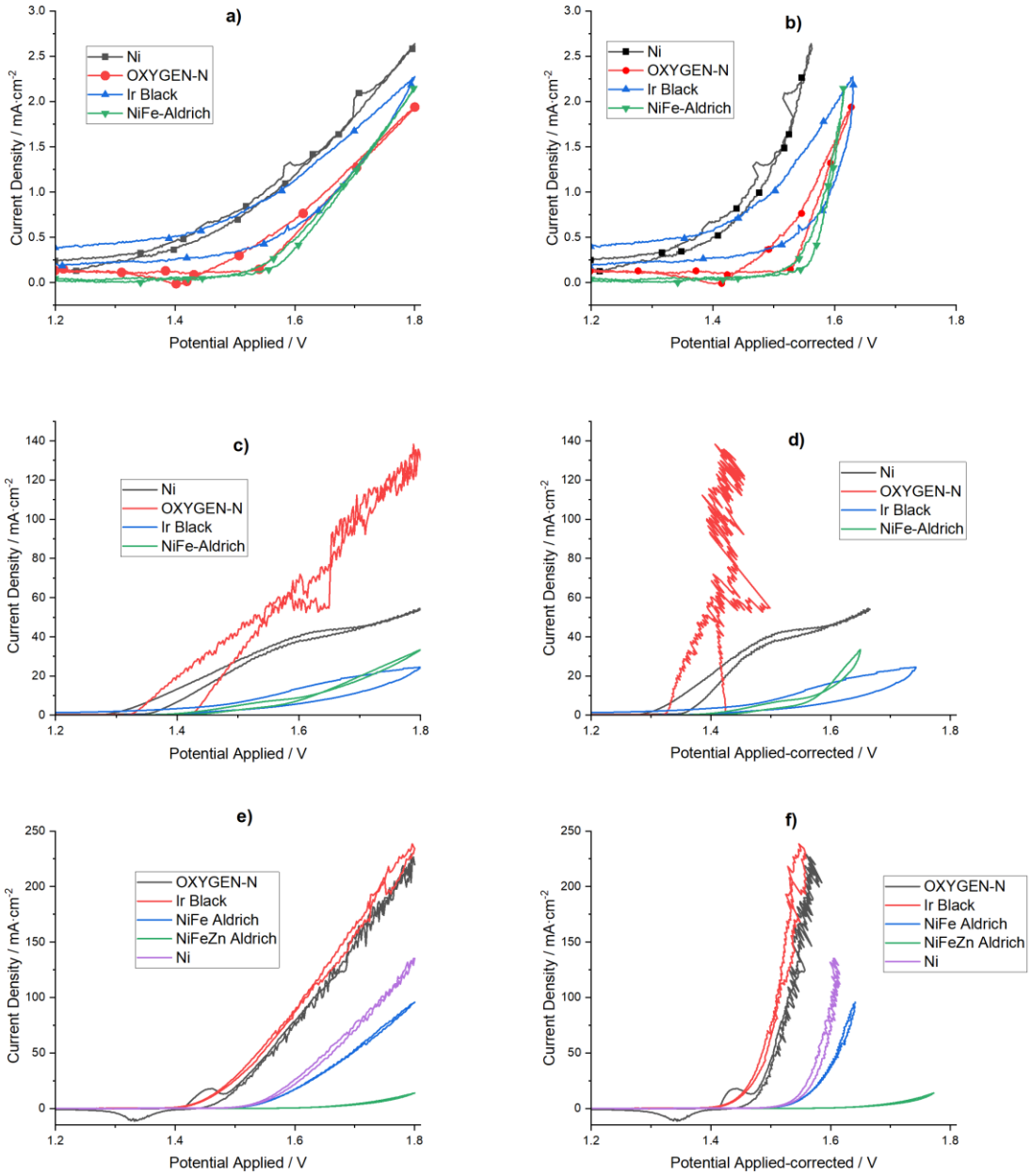

Figure 4.2-Cyclic Voltammetry in RDE (only best cycles are shown) in different electrolytes, studied at room temperature (ca. 20 °C-25 °C). a) and b) are corrected and uncorrected results in pure AdBlue, respectively. c) and d) are the corrected and uncorrected results in

AdBlue + 1 M KOH, respectively and e) and f) are the corrected and uncorrected results in UPW + 1 M KOH, respectively.

Nevertheless, further experiments should be done to understand if this catalyst promotes ammonia production as well as OER and what are the contributions of each reaction. It should also be studied catalyst activity for ammonia oxidation into N_2, H_2 and CO_2 production, something that is not meant to occur in the scope of this project. Ni/Fe ratio can also be studied for this precise end, to understand if it has influence in urea assisted electrolysis.

4.1.3 UPW and KOH *vs* AdBlue and KOH

In Figure 4.3 OXYGEN-N's behavior can be compared in all three electrolytes used. It can clearly be seen an increase of performance when KOH is added to AdBlue. In fact, pure AdBlue performance curve can barely be noticed in the figure with better performance by a factor of 60 (from 2 mA·cm^{-2} to 125 mA·cm^{-2}).

AdBlue + 1 M KOH experiment even obtains better performance than UPW + 1M KOH at lower voltages, with currents being registered at around 1.35 V instead of 1.45 - 1.5 V. AdBlue experiment has even reached 100 mA·cm^{-2} at just above 1.4 V (corrected) while for UPW it only happened above 1.5 V. It is then deduced that OXYGEN-N has high activity in AdBlue with 1 M KOH, more than in UPW but, due to its low conductivity, AdBlue has electrolyte has more ohmic resistances associated which greatly impacts performance.

There is obviously some uncertainty in these results due to the noisy response obtained but it could also correlate to gas bubble formation, without detachment from the electrode surface.

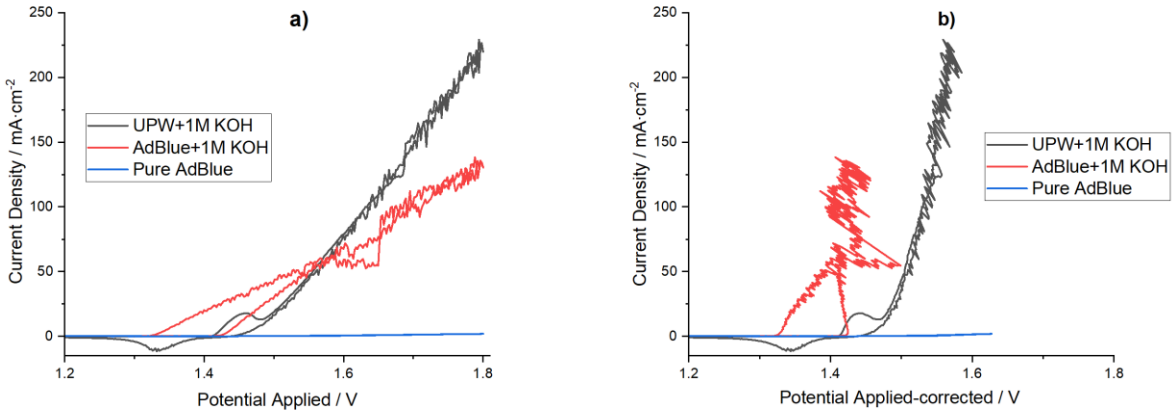

Figure 4.3- Cyclic Voltammetry with RDE coated with OXYGEN-N, different support electrolytes at room temperature (20 °C - 25 °C), a) is the uncorrected plot and b) already corrected.

4.2 Submerged Cells

Cells used during this subchapter are described in the table 3.2 and during result discussion they will be labeled as "SC.x", as presented in the table. Due to high degradation, most cells used in AdBlue were not subjected to KOH concentrations above 0.1 M and so, comparisons between MEAs were done with pure AdBlue or in AdBlue with 0.1 M KOH.

4.2.1 Temperature

Temperature of operation for AEM electrolyzers is a critical point in the development of this technology. PEMWE normal operation occurs at about 80 °C and this is one of the reasons why current densities and durability are much better for this technology. It can be seen, in Fig. 4.4, that this is also true for both supporting electrolytes (AdBlue and UPW) significant performance increases from 50 °C to 70 °C. In Fig. 4.4 a), the test at 70 °C in pure AdBlue shows a peak current density above 60 mA·cm^{-2} whereas tests at 50 °C and 60 °C stayed at 30 mA·cm^{-2}.

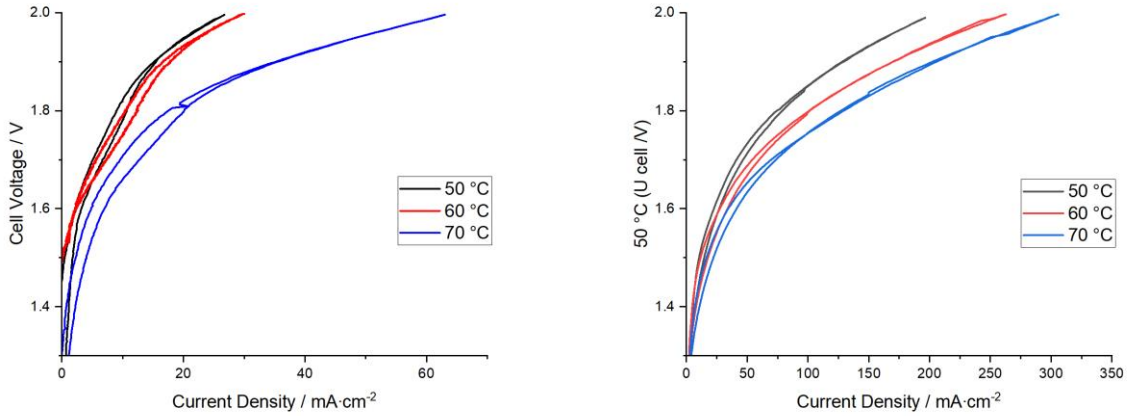

Figure 4.4- I-V Curves at different temperatures for a) SC.4, Sustanion MEA, in Pure AdBlue; b) SC.6, experimental MEA in AdBlue and 1M KOH.

For AdBlue, is important to be aware that water evaporation leads to urea crystals formation. These crystals were appearing recurrently in all three experimental setups used and, even though their influence and impact on the electrolyzer system is not described in any paper to the author's best knowledge, it could certainly lead to MEA degradation and puncture and an overall problematic operation of the system. It was also noted that increase in temperature in AdBlue results in presence of unpleasant smell, possibly due to ammonia formation and this can influence operability. It is important to remind that AEMs presently used still have thermal degradation problems which would lead to lower system lifetime. Other noticeable things during operation in AdBlue include SS rapid passivation and transformation of the electrolyte into a blueish solution. Not a lot of attention was paid to the latter, but it could

be hypothesized that it results from Fe, detached from catalyst, reacting with intermediate species of the reaction.

4.2.2 MEA

As mentioned before, submerged cells were a simpler approach to understand the process of urea/AdBlue electrolysis and the AEMWE system. In this method, MEA, KOH concentrations and temperature are easier to change. For this work, commercial membranes' behavior was one of the main parameters studied. As this system is in its embryonic stage, little information is known about it and there are no membranes directly manufactured for urea/AdBlue electrolysis. Fig. 4.5 shows performance of three different MEAs in study with 3 different membranes, and their performance, in two distinct temperatures and KOH concentrations in AdBlue.

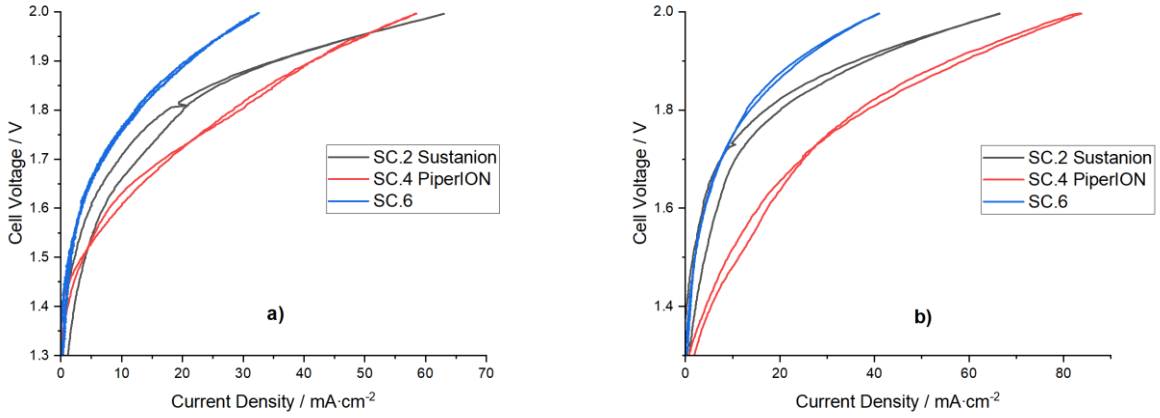

Figure 4.5-I-V curves for 3 MEAs using different membranes (SC 2,4 and 6 in a) pure AdBlue at 70 °C and b) AdBlue with 0.1M KOH at 60 °C.

Membranes used were: PiperION™ A70-HCO3, Sustanion™ X37-50 and an experimental membrane. It is important to mention that for this SC.4, instead of substrates with ionomer from the same brand, PiperION ionomer was used due to material shortage. Regarding the experimental membrane, information about CCS and membrane are undisclosed. Substrates were already prepared by the partner company and just needed special activation steps. In the first case, Fig 4.5 a), tests were run at 70 °C with just AdBlue with low current densities being achieved. Sustanion and PiperION cells obtained almost the same peak current at around 60 mA·cm^{-2} even though the device with PiperION membrane got better performances at lower potentials. The cell with an experimental membrane did not went beyond 30 mA·cm^{-2}. Fig.4.5 b), with AdBlue and 0.1 M KOH at 60 °C, PiperION membrane got much better results and reached 80 mA·cm^{-2} whereas the experimental membrane and Sustanion reached 40 mA·cm^{-2} and 60 mA·cm^{-2} respectively.

It is clear from the results that SC.6 cell had the worst results in both situations. Nonetheless, it was the only MEA to withstand all the test until 1 M KOH, in AdBlue. It needs to be referred that SC.6 cell used higher torques for cell compression than SC.2 and SC.4 (0.6 N·m instead of 0.2 N·m). That could mean that same compression could mean even lower performance.

4.2.3 KOH concentrations in AdBlue *vs* in UPW

In this subchapter there are two main influences from KOH concentrations that were studied. One is the influence of up to 1 M KOH concentrations in AdBlue. To understand that, only SC.6 was used for more than pure AdBlue and AdBlue + 0.1 M KOH. However, components used for this MEA (membrane, and substrates) from the partner company were not used in experiments in UPW+KOH. Because of it, and unfortunately, no full comparison between UPW and AdBlue as supporting electrolytes was not possible for this experimental setup. Fig. 4.6 shows SC.6 electrolyzer's performance with increasingly KOH concentrations in AdBlue.

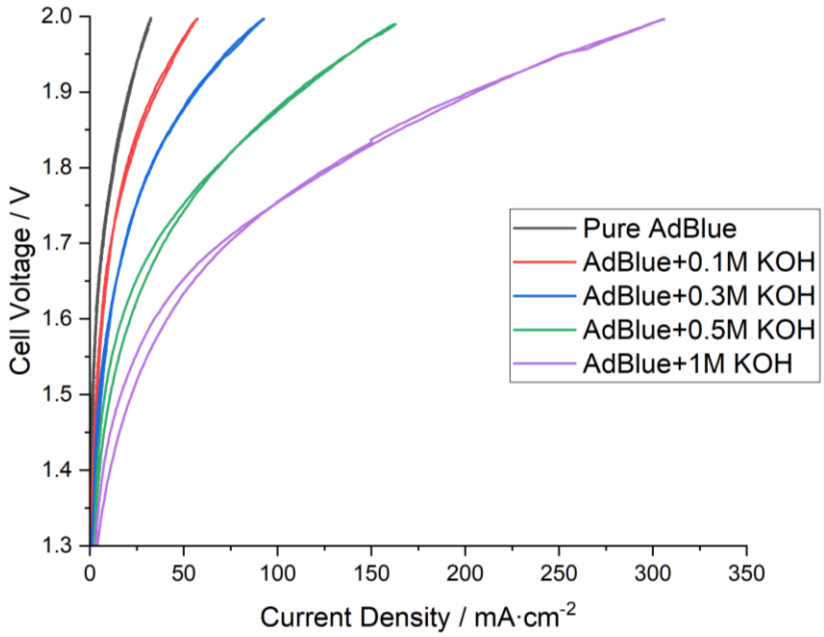

Figure 4.6- I-V curves for SC.6 MEA, in AdBlue with different KOH concentrations, at 70 °C.

In this case, contrary to what has been described for AEMWE [70], there is a clear and major improvement in performance under higher KOH concentrations up to 1 M KOH. It can be observed an increase by 100% from 0.5 M to 1 M (from *ca.* 150 mA·cm^{-2} to 300 mA·cm^{-2}) and more remarkable, an increase in 10 times between pure AdBlue and AdBlue with 1M KOH. There could be several explanations for these results. First, NiOOH formation occurs in much higher rates when OH^- is present. Without NiOOH, catalyst will have poor activity. There is also the possibility of higher concentrations of KOH having such an effect in performance with urea and not with UPW, due to a bigger contribution of the urea hydrolysis reaction. The reason behind this thought is, if KOH concentrations can limit OER in AEMWE, it can mean that in AdBlue

electrolysis UOR replaces and part of OER reaction. It could also mean that the ionomer used has poor ionic conductivity for urea reaction and that performance increases substantially with higher pH due to higher OH^- conductivity. Either way, these current densities are still very poor when compared to other AEMWE results (even though there is not a direct comparison for this MEA). It is difficult to understand what could be the OER's and/or UOR's contribution and if the increase in KOH concentration will lead to an increase in ammonia production.

For comparison between supporting electrolytes, UPW and AdBlue, PiperIONs' MEAs were used (SC.1 in UPW and SC.2 in AdBlue). It must be considered that there is a lack of experiments in high KOH concentrations for AdBlue for this cell. Sustanion's MEA (SC:3 and SC.4) were not used for this comparison because there were considerable differences in substrate (SS *vs* Ni felts), catalysts (Ir Black *vs* NiFeOx) and ionomer (Sustanion' XB-7 *vs* PiperION A-HCO3), respectively for SC.3 and SC.4 has it can be seen in the table 3.2. This can fairly affect the results and lead to difficulties in comparison. Fig. 4.7 shows how 0.1 M KOH in AdBlue compares 0.1M KOH in UPW and, at 50 °C and 60 °C.

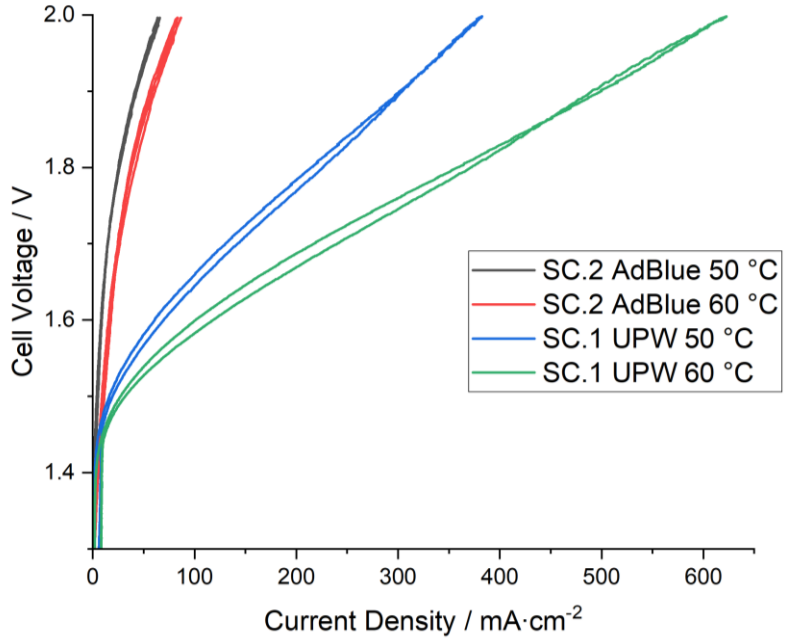

Figure 4.7- I-V curves for SC.1 and SC.2 MEA with UPW and AdBlue as supporting electrolyte with 0.1 M KOH, respectively at 50 °C and 60 °C.

It can be seen how AdBlue, and more specifically the presence of urea hinders better performances from the electrolysis cells. At 60 °C, peak current densities went from $mA{\cdot}cm^{-2}$ in AdBlue to 600 $mA{\cdot}cm^{-2}$ in UPW, at the same KOH concentration. For submerged cells, this could be mainly attributed to mass transport problems, with difficulty for urea to actively move to the catalyst surface. Difficulty of urea hydrolysis reaction to occur also contributes for the low performances.

Finally, it was studied the KOH concentrations' influence in UPW electrolyte for AEMWE Fig. 4.8.

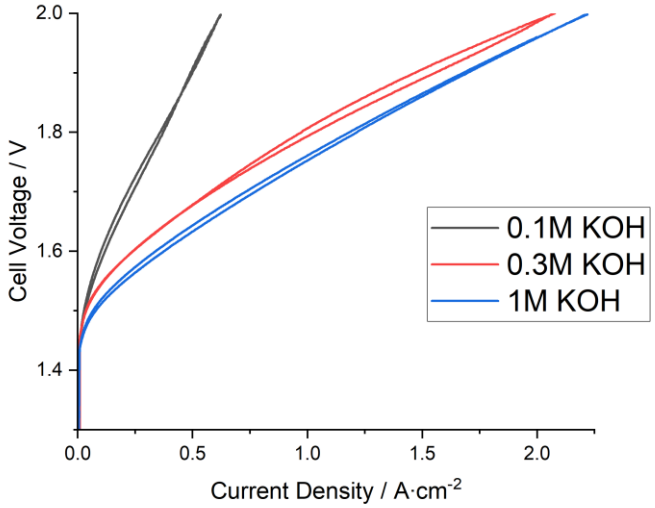

Figure 4.8-I-V curves for SC.2 cell tested in UPW with different KOH Concentrations at 60 °C.

It can be seen, for PiperION MEA SC.1 at 60 °C, that the main increase in performance occurs when concentration increases from 0.1 M to 0.3 M, consistent with literature [70]. From then on, there is low to no improvement in performance, due to an increase in viscosity and mass transport limitations from an increase in gas bubble formation in the catalyst surface. Cell degradation also has to be considered, mainly for higher concentrations, where several tests have already been run and material passivation worsens.

4.2.4 Electrochemical Impedance Spectroscopy

EIS performed in this work were not explored in depth. However, these tests are still valuable for overall reaction comprehension and the resistances associated to it. In an EIS characterization using Nyquist diagram, the point where curve crosses the real frequency axis is the value of the internal ohmic resistances. This includes resistances from electric conduction of BPPs, PTLs, substrates and catalyst layers and, most important ionic conductivity resistance through AEI in the catalyst layer and membrane. The rest of the curves are still difficult to understand for AEMWEs and completely unknown for the electrochemical reaction here suggested. However, they are normally associated to resistances and charge accumulation in some interfaces. Fig. 4.7 exhibits Nyquist plots for comparison of three different parameters, discussed in previous subchapters.

Temperature (Fig. 4.9 a)), does not influence resistance substantial, and between temperatures and it could even be said that 50 °C and 60 °C are practically the same. Nevertheless, 70 °C showed lower ohmic resistance, around 1250 mΩ·cm^2, against 1500 mΩ·cm^2 for 50 °C and 60 °C temperatures. High temperature will increase metal resistance, however,

for electrolyzers, membrane ionic conductivity is much more influential for internal resistance and for this, an increase in temperature improves considerably ion migration and diffusion through the membrane. In terms of dynamic resistance, related to mass transport and activation losses, resistances are very poor, close for 50 °C and 60 °C and much better for 70 °C. Only one curve is distinguished and its estimated value for 70 °C it is around 6750 $m\Omega \cdot cm^2$ and for 50 °C and 60 °C should be around 7500 $m\Omega \cdot cm^2$.

Fig. 4.9 b), there is a different behaviour of the Nyquist plots for higher and lower KOH concentrations. Ohmic resistances are, as expected, inversely proportional to KOH concentrations. The best-case scenario is AdBlue with 1 M KOH with an Ohmic resistance little below 500 $m\Omega \cdot cm^2$. In pure AdBlue, an ohmic resistance *ca.* 1250 $\Omega \cdot cm^2$ explains part of the low performance in this electrolyte. This steep difference explained by the increase in ionic conduction through the catalyst layer and membrane. However, and less clear, are the Nyquist curves that could be identified. For concentrations equal or above 0.3 M, there is a subtle change in curvature at higher frequencies, sooner on the x axis (only 1 M KOH scenario is represented in text). This will probably mean that there are to different phenomena that originate to separate resistances, one at lower frequencies, which is dominant, and one at higher frequencies. The latter, for AdBlue with low to no concentrations, is completely overshadowed by the main phenomena. It could be assumed that the first curve probably represents the HER reaction while the main bigger curve is attributed to OER/UOR reactions. For 1 M KOH curve it could be estimated that first resistance at higher frequencies has a value around 1500 $m\Omega \cdot cm^2$ and for lower resistance stands around 4500 $m\Omega \cdot cm^2$.

Finally, Figure 4.9 c) shows how AdBlue, as the support electrolyte replacing water, can be so much worst. Ohmic resistance for water with KOH situate around 250 $m\Omega \cdot cm^2$ while for AdBlue with the same KOH concentration has around, 1300 $m\Omega \cdot cm^2$. This is an astonishing difference, and it could be related to lower AdBlue ionic conductivity. Respecting other resistances, cell with water as electrolyte has a fixed semi-circle, that should be connected to the anodic reaction, with a value of around 1250 $m\Omega \cdot cm^2$. For AdBlue, it looks like there could be two superimposed semicircles, as it was seen in Fig. 4.9 b). It is difficult to separate and attribute values for both resistances but together, they should exceed 4 $\Omega \cdot cm^2$.

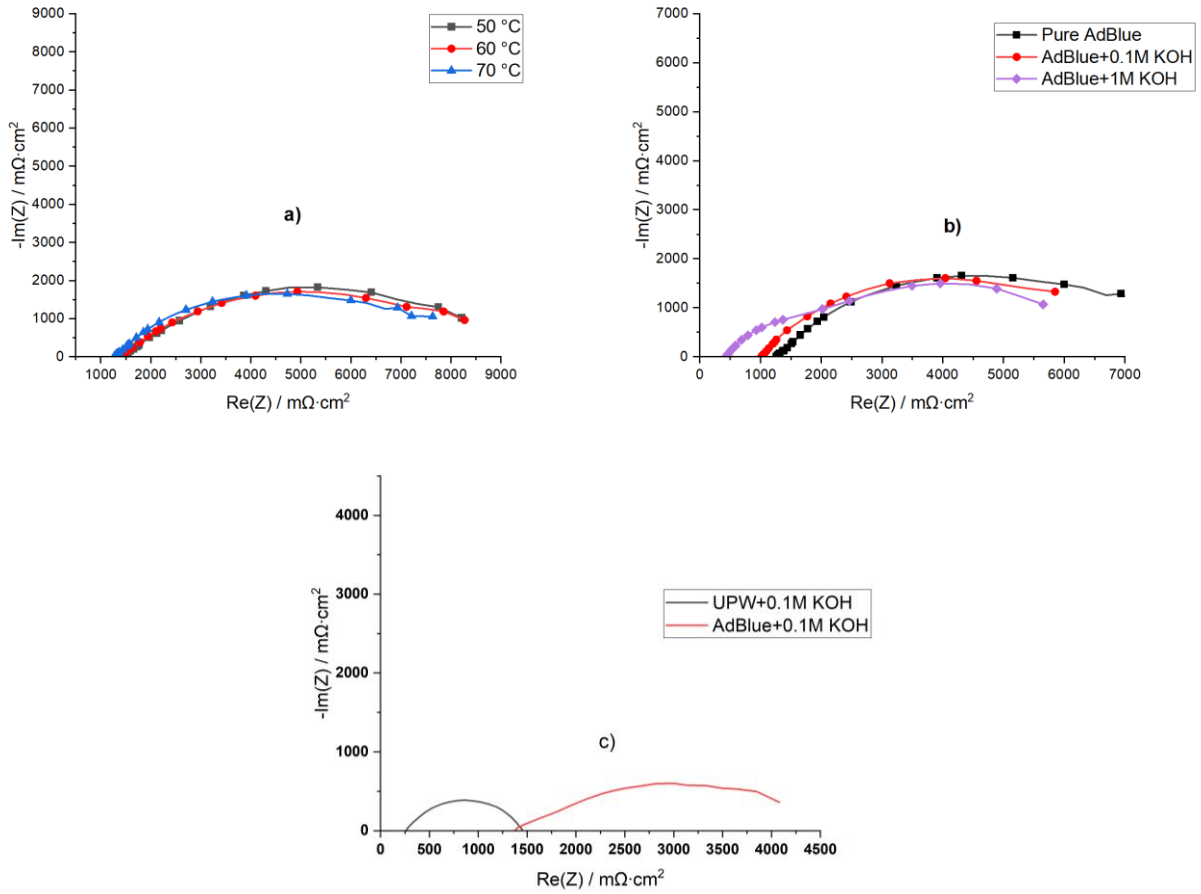

Figure 4.9- EIS displayed as Nyquist plot; In a) curves obtained at 1 M KOH in AdBlue for SC.6; at different temperatures b) SC.6 in AdBlue with different KOH concentrations at 70 °C and c) SC.3 and SC.4 in UPW and AdBlue, respectively, with 0.1 M KOH at 70 °C.

4.3 Closed Cell

Closed single cell testing is the closer thing to a commercially available solution, in this work. As mentioned before, these test bench will function with feeding solutions for anode and cathode at different flow rates. Due to time constraints, in this thesis only a glimpse of closed single cells is done. Further optimization and durability tests should be done. Moreover, gas chromatography analysis on both anodic and cathodic electrolytes must be performed for a better understanding of the real H_2 and NH_3 production by the cell. Specifications of the cells used in this experimental setup can be found in Table 3.3

4.3.1 Torque and Flow rate optimization

A first approach to this test bench was done with cell compression feed flow rate optimization using 0.1M KOH electrolyte and CC.0. Results here can help to outline operating conditions for this test bench but they are closely related to the materials used, like substrates/PTL and membranes, and so, tests for each MEA should be done. Fig.4.10 shows how torque and cathode's side flow rate influence cell performance, at 60 °C.

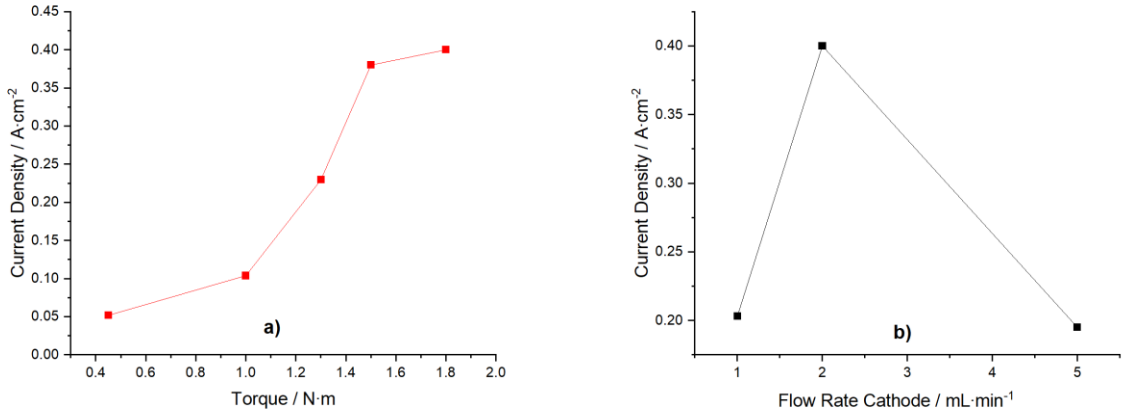

Figure 4.10-Peak current density as a function of torque used for submerged cell compression in a) as a function of the cathode flow rate in b). Measurements were done at 60 °C and 2 mL·min^{-1} anode flow rate.

It can be seen, as expected, that peak current density increases with torque used for MEA compression. However, what was not expected was the MEA to endure such high compressions, up to 1.8 N·m, without puncturing the membrane and subsequent short circuit. As it could later be seen, MEAs used for AdBlue can even endure torques up to 2.2 N·m without compromising membrane integrity. Relating to flow rate, only cathode side was studied due to fast membrane degradation over time. It is well documented that dry cathode side of AEMWE and PEMWE can be the optimal operating condition for this electrode since it creates a the best environment for high-purity, dry H_2 [72]. However, and due to AEM degradation when dry, measurements were always done with feeding electrolyte. During this test, it was observed that 2 mL·min^{-1} achieved the best peak current density and thus it will be used in the following experiments. Anodic feeding solution, if in low flow rates, will also help with H_2 removal from the electrode and thus increasing performance. For the anode side, and consulting literature, it was stablished that flow rate should remain at 40 mL·min^{-1}. Anodic feeding solution will be the main reactant source for this reaction. High flow rate will enable better water's and AdBlue's intake and it will help with gas removal from the system. However, there is a limit from where the limiting phenomena will be mass transport and no significant increases will be noticeable.

4.3.2 KOH Influence

In closed cell, as in submerged cell, KOH concentration influence was studied when using AdBlue (Fig. 4.11). KOH concentrations of 0.1 M, 1 M as well as pure AdBlue were tested. Here it can be seen the influence of KOH in both a CCM and CCS MEAs.

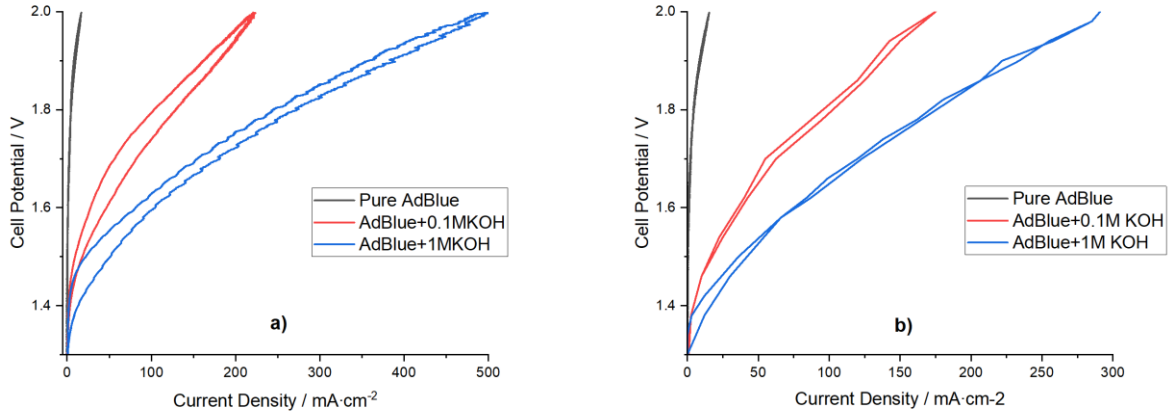

Figure 4.11- I-V curves of two closed electrolyzer cells in AdBlue with different KOH concentrations. In a), CC.1 (experimental CCS) was used, and b) CC.3 (CCM-Fumatech). Tests run at 60 °C, 40 and 2 mL·min^{-1} flow for cathode and anode respectively.

Increase in KOH concentration, for this setup, has the same kind of influence previously observed for submerged cells, higher concentrations in AdBlue will massively increase performance. Very significant increases between pure AdBlue as electrolyte and AdBlue with 1 M KOH are observed for both CCM and CCS. For CCS, performance increases from 17 mA·cm^{-2} to 500 mA·cm^{-2} and 15 mA·cm^{-2} to 275 mA·cm^{-2} for CCM prove the importance of KOH for this system. However, these substantial increases are no related to good cell performances in AdBlue with 1 M KOH but rather very disappointing current densities when only AdBlue is used.

4.3.3 CCM *vs* CCS *vs* CCM-CCS

As aforementioned, the three types of electrode coating were studied in this closed continuous cell set-up. Materials used for each cell were different, mainly membranes. This could lead to misleading interpretation of the optimal method. Fig. 4.12 shows how the cells performed with AdBlue and 1M KOH, at 60 °C.

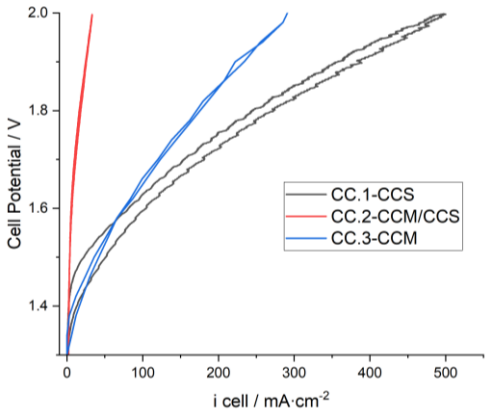

Figure 4.12- I-V curves for the three different MEAs, in AdBlue with 1 M KOH at the operating conditions previously mentioned in 4.11.

Results suggest improved performance for the CCS MEA, much better than CCM one. CCS MEA reaches almost double the current density of CCM (500 $mA \cdot cm^{-2}$ *vs.* 300 $mA \cdot cm^{-2}$) despite showing some thermal stability issues (difference between forwards and reverse curves). Mixed coating technique (CCS/CCM) approach showed a clearly poorer performance when compared to the other techniques (only 30 $mA \cdot cm^{-2}$). The most reasonable explanation for these results is membrane integrity after catalyst coating. It is important to remind that these membranes are both mechanically and chemically unstable. Overflowing, even if minor one, can have severe consequences like membrane tear and rupture. Moreover, substrates have the possibility of being hot pressed after catalyst coating. This will provide better contact between catalytic layer and substrate surface, hindering catalyst detachment.

Comparison between different coating approaches employing the same membrane will lead to better understanding of these techniques and their influence on performance. Nevertheless, Fumatechs' membranes seem to perform much better than Sustanion ones, when coated. Moreover, and due to their low-cost, membranes from Fumatech could be the most feasible.

5 Conclusion

An innovative technology for converting AdBlue (urea and water) into ammonia and hydrogen using an electrochemical device, anion exchange membrane electrolyzer, was tested. Several components of the AEM electrolyzer were studied, namely the anion exchange membranes and ionomers, the catalyst for the anodic reaction, substrates and porous transport layers. Concerning the use of submerged cells, several membranes were tested with potential controlled cycles and EIS with both AdBlue and water, with KOH, and at 50 °C, 60°C and 70 °C. A rotating disk electrode (RDE) was also used for assessing the electrochemical catalytic activity, mainly when using pure AdBlue and AdBlue with 1 M KOH. Finally, a closed electrolyzer was used with AdBlue and three different catalyst coating techniques were assessed, CCM, CCS and CCM/CCS.

In submerged cells, only the cell using the experimental MEA endured all KOH concentrations tested in AdBlue, from 0.1 M up to 1 M; a current density of 300 $mA \cdot cm^{-2}$ was reached for this cell at 2 V, 70 °C with 1 M KOH. Compared with the best performance obtained in water electrolysis with 1 M KOH, 4 $A \cdot cm^{-2}$, for the same temperature and using the PiperION MEA, AdBlue electrolysis is still far away from those values. In RDE, OXYGEN-N catalyst from the experimental showed indisputably the best performance for the electrolysis of AdBlue with 1 M KOH, 125 $mA \cdot cm^{-2}$. It was even concluded that activity from OXYGEN-N is higher in AdBlue than in UPW, with 1 M KOH. However, due to high ohmic resistances, peak current density at 1.8 V is still higher for UPW with 1 M KOH, ca. 225 $mA \cdot cm^{-2}$ vs. 125 $mA \cdot cm^{-2}$ in AdBlue + 1 M KOH. Catalytic activity using pure AdBlue was really poor and performances were similar for all tested catalysts, with current densities below 3 $mA \cdot cm^{-2}$. Performances in a closed electrolyzer cell were much higher than those in submerged cells, with experimental CCS MEA reaching close to 500 $mA \cdot cm^{-2}$ at 2 V, 60 °C in AdBlue with 1 M KOH. A CCM, using Fumatech membrane, was developed and despite having lower performance than the experimental CCS, reached interesting values of current density, close to 250 $mA \cdot cm^{-2}$. Performances in pure AdBlue were also poor for this experimental setup, around 15 – 20 $mA \cdot cm^{-2}$

This work enabled further development of the state of the art for this innovative approach that is being developed as an alternative to SCR for reduction of NOx emissions. Current densities achieved are still very poor, but OXYGEN-N catalyst showed high electrocatalytic activity on AdBlue with KOH. Nonetheless, Performances are still falling short due to mass transport and ohmic resistance problems. An increase of temperature could improve mass transport kinetics and decrease ohmic resistances from the membrane but for that, more stable membranes must be developed. The research should proceed and the stability should be addressed as well as the composition of evolved gases.

6 Assessment of the work done

6.1 Objectives Achieved

The main objectives for this work included were to study the behaviour of several AEMWE components for urea conversion into ammonia (using AdBlue) and try to find the best possible combination. Catalysts studied in RDE helped understand electrocatalytic activity and OXYGEN-N from CENmat was found to be the best one. Moreover, this catalyst has shown better electrochemical activity in AdBlue with 1 M KOH than in UPW with 1 M KOH. However, AdBlue lack of conductivity and ohmic resistance leads to the worst peak current densities.

In submerged cells, several membranes were tested, and some results were obtained to help understand the main problems for AdBlue electrolysis. It was found that several commercial membranes cannot withstand many experiments in AdBlue without degrading. The experimental MEA (with membrane and anode/cathode coated substrate) from a partner company provided a consistent cell that was durable throughout every temperature and concentration of KOH in AdBlue.

Finally, for closed cells, the main objective was to study a device, closer to a possible future commercial apparatus, in AdBlue. CCM and CCS techniques were also studied. Results show an increase in performance for higher KOH concentrations for closed cells when compared to submerged cell. Operating conditions like torque and flow rates were also optimized. The experimental CCS outperformed the developed CCM with Fumatech's membrane. This cell with CCS MEA reached 0.5 $A \cdot cm^{-2}$ that, while a very respectable performance, problems with mass transport losses and ohmic losses still have to be solved. Unfortunately, gas chromatography was not used, nor durability and EIS tests were done on these cells and should be a priority moving forward.

6.2 Final Assessment

The work developed, while not a complete success, was very insightful for a technology that is still puzzling and in an early stage of development. Working in several testing methods enabled me to better understand several matters such as anion exchange membrane electrolysis and electrocatalyst behavior and activity. The knowledge acquired will help not only for the technology here described but also for all other electrochemical devices and technologies using electrocatalysts.

The author suggests further developments that could still been done. On the RDE setup, studying more transition metals mixed with the NiFe catalyst, different temperatures, different

purging gases (with the proper precautions) and different loadings. Diffusion coefficient for reactions in AdBlue and AdBlue with KOH should also be measured through the Levich's equation [75]. Durability tests should also be carried out.

The author suggests that in both closed cell and submerged cell setup, plenty of other parameters could be studied. More commercially available ionomer/membrane pairs can be tested, ionomer mass content could be changed for both anode and cathode.

Finally, and as the main point, the author believes that in order to have a respectable stack solution for mobile applications, temperature at which the reaction occurs should be increased. While this would bring better performances on the short term, membrane thermal stability would be a limiting factor.

7 References

1. WHO, W.H.O. *What are the WHO Air quality guidelines?* 2021 9/06/2023]; Available from: https://www.who.int/news-room/feature-stories/detail/what-are-the-who-air-quality-guidelines.
2. Achakulwisut, P., M. Brauer, P. Hystad, and S.C. Anenberg, *Global, national, and urban burdens of paediatric asthma incidence attributable to ambient NO(2) pollution: estimates from global datasets*. (2542-5196 (Electronic)).
3. Halleux, V. Development of Euro 7 Emission Standards for Cars, Vans, Lorries and Buses 2023, European Parliament: https://www.europarl.europa.eu/legislative-train/carriage/post-euro6vi-emission-standards/report
4. White, L., A. Miles, C. Boocock, and J.-G.M. Cooper, Stephen. EURO 7 IMPACT ASSESSMENT: THE OUTLOOK FOR AIR QUALITY COMPLIANCE IN THE EU AND THE ROLE OF THE ROAD TRANSPORT SECTOR 2021, Aeris Europe: https://aeriseurope.com/papers-and-articles/euro-7-impact-assessment-the-outlook-for-air-quality-compliance-in-the-eu-and-the-role-of-the-road-transport-sector/
5. Hountalas, D.T., G.C. Mavropoulos, and K.B. Binder, *Effect of exhaust gas recirculation (EGR) temperature for various EGR rates on heavy duty DI diesel engine performance and emissions*. Energy, 2008. **33**(2): p. 272-283.
6. IEA, 2021, Global installed electrolysis capacity by technology, 2015-2020, Paris: https://www.iea.org/data-and-statistics/charts/global-installed-electrolysis-capacity-by-technology-2015-2020
7. Paygozar, S., A. Sabour Rouh Aghdam, E. Hassanizadeh, R. Andaveh, and G. Barati Darband, *Recent progress in non-noble metal-based electrocatalysts for urea-assisted electrochemical hydrogen production*. International Journal of Hydrogen Energy, 2023. **48**(20): p. 7219-7259.
8. Rapp, V., N. Killingsworth, P. Therkelsen, and R. Evans, *4 - Lean-Burn Internal Combustion Engines*, in *Lean Combustion (Second Edition)*, Derek Dunn-Rankin and Peter Therkelsen, Editors. 2016, Academic Press: Boston. p. 111-146.
9. Zhen, X., Y. Wang, S. Xu, Y. Zhu, C. Tao, T. Xu, and M. Song, *The engine knock analysis – An overview*. Applied Energy, 2012. **92**: p. 628-636.
10. Heywood, J.B., *Internal combustion engine fundamentals*, ed. MCGraw Hill. 1988.
11. Hill, S.C. and L. Douglas Smoot, *Modeling of nitrogen oxides formation and destruction in combustion systems*. Progress in Energy and Combustion Science, 2000. **26**(4): p. 417-458.
12. Hoekman, S.K. and C. Robbins, *Review of the effects of biodiesel on NOx emissions*. Fuel Processing Technology, 2012. **96**: p. 237-249.
13. Busca, G., L. Lietti, G. Ramis, and F. Berti, *Chemical and mechanistic aspects of the selective catalytic reduction of NOx by ammonia over oxide catalysts: A review*. Applied Catalysis B: Environmental, 1998. **18**(1): p. 1-36.
14. Reşitoğlu, İ.A., K. Altinişik, and A. Keskin, *The pollutant emissions from diesel-engine vehicles and exhaust aftertreatment systems*. Clean Technologies and Environmental Policy, 2015. **17**(1): p. 15-27.
15. Lowell, D.K., Fanta Urban off-cycle NOx emissions from Euro IV/V trucks and buses- Problems and solutions for Europe and developing countries 2012, ICCT- International council on clean transportation: https://theicct.org/wp-content/uploads/2021/06/ICCT_WP18_urban_Nox_emissions.pdf

16. Koebel, M., M. Elsener, and M. Kleemann, *Urea-SCR: a promising technique to reduce NOx emissions from automotive diesel engines*. Catalysis Today, 2000. **59**(3): p. 335-345.

17. Zhu, H., L. Song, K. Li, R. Wu, W. Qiu, and H. He *Low-Temperature SCR Catalyst Development and Industrial Applications in China*. Catalysts, 2022. **12**, DOI: 10.3390/catal12030341.

18. Abu-Hamdeh, N.H., *Effect of cooling the recirculated exhaust gases on diesel engine emissions*. Energy Conversion and Management, 2003. **44**(19): p. 3113-3124.

19. Zare, A., T.A. Bodisco, M. Jafari, P. Verma, L. Yang, M. Babaie, M.M. Rahman, A. Banks, Z.D. Ristovski, R.J. Brown, and S. Stevanovic, *Cold-start NOx emissions: Diesel and waste lubricating oil as a fuel additive*. Fuel, 2021. **286**: p. 119430.

20. Praveena, V. and M.L.J. Martin, *A review on various after treatment techniques to reduce NOx emissions in a CI engine*. Journal of the Energy Institute, 2018. **91**(5): p. 704-720.

21. Botte, G.G., *Electrolytic Cells and Methods for the Production of Ammonia and Hydrogen*. 2008, Ohio University, Athens, OH (US): United States.

22. Daramola, D.A., D. Singh, and G.G. Botte, *Dissociation Rates of Urea in the Presence of NiOOH Catalyst: A DFT Analysis*. The Journal of Physical Chemistry A, 2010. **114**(43): p. 11513-11521.

23. Suárez, D., N. Díaz, and K.M. Merz, *Ureases: Quantum Chemical Calculations on Cluster Models*. Journal of the American Chemical Society, 2003. **125**(50): p. 15324-15337.

24. Savva, P.G. and C.N. Costa, *Hydrogen Lean-DeNOx as an Alternative to the Ammonia and Hydrocarbon Selective Catalytic Reduction (SCR)*. Catalysis Reviews, 2011. **53**(2): p. 91-151.

25. Lu, F. and G.G. Botte, *Electrochemically Induced Conversion of Urea to Ammonia*. ECS Electrochemistry Letters, 2015. **4**(10): p. E5.

26. Katzer, J.R. *Kinetics of NO Reduction by NH3 over Supported Pt and the Effect of SO2*. in *The Catalytic Chemistry of Nitrogen Oxides*. 1975. Boston, MA: Springer US.

27. Eßer, E., K. Müller, and S. Kureti, *Low-Temperature H2-deNOx in Diesel Exhaust*. Topics in Catalysis, 2022.

28. *Analyze Results: ''Anion exchange membrane'' ''water'' ''electrolysis'' Publication years*. 2023: Web of Science.

29. Du, N., C. Roy, R. Peach, M. Turnbull, S. Thiele, and C. Bock, *Anion-Exchange Membrane Water Electrolyzers*. Chemical Reviews, 2022. **122**(13): p. 11830-11895.

30. Zakaria, Z. and S.K. Kamarudin, *A review of alkaline solid polymer membrane in the application of AEM electrolyzer: Materials and characterization*. International Journal of Energy Research, 2021. **45**(13): p. 18337-18354.

31. Gambou, F., D. Guilbert, M. Zasadzinski, and H. Rafaralahy *A Comprehensive Survey of Alkaline Electrolyzer Modeling: Electrical Domain and Specific Electrolyte Conductivity*. Energies, 2022. **15**, DOI: 10.3390/en15093452.

32. Vincent, I. and D. Bessarabov, *Low cost hydrogen production by anion exchange membrane electrolysis: A review*. Renewable and Sustainable Energy Reviews, 2018. **81**: p. 1690-1704.

33. Bermudez, J.M.E., Stavroula; Pavan, Francesco Electrolysers 2022, IEA: https://www.iea.org/reports/electrolysers

34. Hagesteijn, K.F.L., S. Jiang, and B.P. Ladewig, *A review of the synthesis and characterization of anion exchange membranes*. Journal of Materials Science, 2018. **53**(16): p. 11131-11150.

35. You, W., K.J.T. Noonan, and G.W. Coates, *Alkaline-stable anion exchange membranes: A review of synthetic approaches*. Progress in Polymer Science, 2020. **100**: p. 101177.

36. Chatenet, M., B.G. Pollet, D.R. Dekel, F. Dionigi, J. Deseure, P. Millet, R.D. Braatz, M.Z. Bazant, M. Eikerling, I. Staffell, P. Balcombe, Y. Shao-Horn, and H. Schäfer, *Water electrolysis: from textbook knowledge to the latest scientific strategies and industrial developments*. Chemical Society Reviews, 2022. **51**(11): p. 4583-4762.

37. Arges, C.G., V.K. Ramani, and P.N. Pintauro, *The Chalkboard: Anion Exchange Membrane Fuel Cells*. The Electrochemical Society Interface, 2010. **19**(2): p. 31.

38. Seh, Z.W., J. Kibsgaard, C.F. Dickens, I. Chorkendorff, J.K. Nørskov, and T.F. Jaramillo, *Combining theory and experiment in electrocatalysis: Insights into materials design*. Science, 2017. **355**(6321): p. eaad4998.

39. Kreider, M.E. and M. Burke Stevens, *Material Changes in Electrocatalysis: An In Situ/Operando Focus on the Dynamics of Cobalt-Based Oxygen Reduction and Evolution Catalysts*. ChemElectroChem, 2023. **10**(3): p. e202200958.

40. Liu, L., W. Li, X. He, J. Yang, and N. Liu, *In Situ/Operando Insights into the Stability and Degradation Mechanisms of Heterogeneous Electrocatalysts*. Small, 2022. **18**(7): p. 2104205.

41. Lee, S.A., J. Kim, K.C. Kwon, S.H. Park, and H.W. Jang, *Anion exchange membrane water electrolysis for sustainable large-scale hydrogen production*. Carbon Neutralization, 2022. **1**(1): p. 26-48.

42. Sheng, W., H.A. Gasteiger, and Y. Shao-Horn, *Hydrogen Oxidation and Evolution Reaction Kinetics on Platinum: Acid vs Alkaline Electrolytes*. Journal of The Electrochemical Society, 2010. **157**(11): p. B1529.

43. Ahn, S.H., B.-S. Lee, I. Choi, S.J. Yoo, H.-J. Kim, E. Cho, D. Henkensmeier, S.W. Nam, S.-K. Kim, and J.H. Jang, *Development of a membrane electrode assembly for alkaline water electrolysis by direct electrodeposition of nickel on carbon papers*. Applied Catalysis B: Environmental, 2014. **154-155**: p. 197-205.

44. Subbaraman, R., D. Tripkovic, D. Strmcnik, K.-C. Chang, M. Uchimura, A.P. Paulikas, V. Stamenkovic, and N.M. Markovic, *Enhancing Hydrogen Evolution Activity in Water Splitting by Tailoring Li+-Ni(OH)2-Pt Interfaces*. Science, 2011. **334**(6060): p. 1256-1260.

45. Xue, S., R.W. Haid, R.M. Kluge, X. Ding, B. Garlyyev, J. Fichtner, S. Watzele, S. Hou, and A.S. Bandarenka, *Enhancing the Hydrogen Evolution Reaction Activity of Platinum Electrodes in Alkaline Media Using Nickel–Iron Clusters*. Angewandte Chemie International Edition, 2020. **59**(27): p. 10934-10938.

46. Cao, Z., Q. Chen, J. Zhang, H. Li, Y. Jiang, S. Shen, G. Fu, B.-a. Lu, Z. Xie, and L. Zheng, *Platinum-nickel alloy excavated nano-multipods with hexagonal close-packed structure and superior activity towards hydrogen evolution reaction*. Nature Communications, 2017. **8**(1): p. 15131.

47. Badrnezhad, R., F. Nasri, H. Pourfarzad, and S.K. Jafari, *Effect of iron on Ni–Mo–Fe composite as a low-cost bifunctional electrocatalyst for overall water splitting*. International Journal of Hydrogen Energy, 2021. **46**(5): p. 3821-3832.

48. McKone, J.R., B.F. Sadtler, C.A. Werlang, N.S. Lewis, and H.B. Gray, *Ni–Mo Nanopowders for Efficient Electrochemical Hydrogen Evolution*. ACS Catalysis, 2013. **3**(2): p. 166-169.

49. Zhai, L., T.W. Benedict Lo, Z.-L. Xu, J. Potter, J. Mo, X. Guo, C.C. Tang, S.C. Edman Tsang, and S.P. Lau, *In Situ Phase Transformation on Nickel-Based Selenides for Enhanced Hydrogen Evolution Reaction in Alkaline Medium.* ACS Energy Letters, 2020. **5**(8): p. 2483-2491.

50. Friebel, D., M.W. Louie, M. Bajdich, K.E. Sanwald, Y. Cai, A.M. Wise, M.-J. Cheng, D. Sokaras, T.-C. Weng, R. Alonso-Mori, R.C. Davis, J.R. Bargar, J.K. Nørskov, A. Nilsson, and A.T. Bell, *Identification of Highly Active Fe Sites in (Ni,Fe)OOH for Electrocatalytic Water Splitting.* Journal of the American Chemical Society, 2015. **137**(3): p. 1305-1313.

51. Long, X., S. Xiao, Z. Wang, X. Zheng, and S. Yang, *Co intake mediated formation of ultrathin nanosheets of transition metal LDH—an advanced electrocatalyst for oxygen evolution reaction.* Chemical Communications, 2015. **51**(6): p. 1120-1123.

52. Xu, D., M.B. Stevens, M.R. Cosby, S.Z. Oener, A.M. Smith, L.J. Enman, K.E. Ayers, C.B. Capuano, J.N. Renner, N. Danilovic, Y. Li, H. Wang, Q. Zhang, and S.W. Boettcher, *Earth-Abundant Oxygen Electrocatalysts for Alkaline Anion-Exchange-Membrane Water Electrolysis: Effects of Catalyst Conductivity and Comparison with Performance in Three-Electrode Cells.* ACS Catalysis, 2019. **9**(1): p. 7-15.

53. Cossar, E., F. Murphy, and E.A. Baranova, *Nickel-based anodes in anion exchange membrane water electrolysis: a review.* Journal of Chemical Technology & Biotechnology, 2022. **97**(7): p. 1611-1624.

54. Anantharaj, S., S. Kundu, and S. Noda, *"The Fe Effect": A review unveiling the critical roles of Fe in enhancing OER activity of Ni and Co based catalysts.* Nano Energy, 2021. **80**: p. 105514.

55. Zhang, N., X. Feng, D. Rao, X. Deng, L. Cai, B. Qiu, R. Long, Y. Xiong, Y. Lu, and Y. Chai, *Lattice oxygen activation enabled by high-valence metal sites for enhanced water oxidation.* Nature Communications, 2020. **11**(1): p. 4066.

56. Bodhankar, P.M., P.B. Sarawade, G. Singh, A. Vinu, and D.S. Dhawale, *Recent advances in highly active nanostructured NiFe LDH catalyst for electrochemical water splitting.* Journal of Materials Chemistry A, 2021. **9**(6): p. 3180-3208.

57. Gong, M., Y. Li, H. Wang, Y. Liang, J.Z. Wu, J. Zhou, J. Wang, T. Regier, F. Wei, and H. Dai, *An Advanced Ni–Fe Layered Double Hydroxide Electrocatalyst for Water Oxidation.* Journal of the American Chemical Society, 2013. **135**(23): p. 8452-8455.

58. Park, J.E., S.Y. Kang, S.-H. Oh, J.K. Kim, M.S. Lim, C.-Y. Ahn, Y.-H. Cho, and Y.-E. Sung, *High-performance anion-exchange membrane water electrolysis.* Electrochimica Acta, 2019. **295**: p. 99-106.

59. Vincent, I., A. Kruger, and D. Bessarabov, *Development of efficient membrane electrode assembly for low cost hydrogen production by anion exchange membrane electrolysis.* International Journal of Hydrogen Energy, 2017. **42**(16): p. 10752-10761.

60. Koch, S., P.A. Heizmann, S.K. Kilian, B. Britton, S. Holdcroft, M. Breitwieser, and S. Vierrath, *The effect of ionomer content in catalyst layers in anion-exchange membrane water electrolyzers prepared with reinforced membranes (Aemion+™).* Journal of Materials Chemistry A, 2021. **9**(28): p. 15744-15754.

61. Li, D., E.J. Park, W. Zhu, Q. Shi, Y. Zhou, H. Tian, Y. Lin, A. Serov, B. Zulevi, E.D. Baca, C. Fujimoto, H.T. Chung, and Y.S. Kim, *Highly quaternized polystyrene ionomers for high performance anion exchange membrane water electrolysers.* Nature Energy, 2020. **5**(5): p. 378-385.

62. Huang, G., M. Mandal, N.U. Hassan, K. Groenhout, A. Dobbs, W.E. Mustain, and P.A. Kohl, *Ionomer Optimization for Water Uptake and Swelling in Anion Exchange Membrane Electrolyzer: Oxygen Evolution Electrode.* Journal of The Electrochemical Society, 2020. **167**(16): p. 164514.

63. Faid, A.Y., L. Xie, A.O. Barnett, F. Seland, D. Kirk, and S. Sunde, *Effect of anion exchange ionomer content on electrode performance in AEM water electrolysis.* International Journal of Hydrogen Energy, 2020. **45**(53): p. 28272-28284.

64. Huang, G., M. Mandal, N.U. Hassan, K. Groenhout, A. Dobbs, W.E. Mustain, and P.A. Kohl, *Ionomer Optimization for Water Uptake and Swelling in Anion Exchange Membrane Electrolyzer: Hydrogen Evolution Electrode.* Journal of The Electrochemical Society, 2021. **168**(2): p. 024503.

65. Miller, H.A., K. Bouzek, J. Hnat, S. Loos, C.I. Bernäcker, T. Weißgärber, L. Röntzsch, and J. Meier-Haack, *Green hydrogen from anion exchange membrane water electrolysis: a review of recent developments in critical materials and operating conditions.* Sustainable Energy & Fuels, 2020. **4**(5): p. 2114-2133.

66. Carmo, M., D.L. Fritz, J. Mergel, and D. Stolten, *A comprehensive review on PEM water electrolysis.* International Journal of Hydrogen Energy, 2013. **38**(12): p. 4901-4934.

67. Xu, Q., L. Zhang, J. Zhang, J. Wang, Y. Hu, H. Jiang, and C. Li, *Anion Exchange Membrane Water Electrolyzer: Electrode Design, Lab-Scaled Testing System and Performance Evaluation.* EnergyChem, 2022. **4**(5): p. 100087.

68. Lim, A., H.-j. Kim, D. Henkensmeier, S. Jong Yoo, J. Young Kim, S. Young Lee, Y.-E. Sung, J.H. Jang, and H.S. Park, *A study on electrode fabrication and operation variables affecting the performance of anion exchange membrane water electrolysis.* Journal of Industrial and Engineering Chemistry, 2019. **76**: p. 410-418.

69. Stiber, S., H. Balzer, A. Wierhake, F.J. Wirkert, J. Roth, U. Rost, M. Brodmann, J.K. Lee, A. Bazylak, W. Waiblinger, A.S. Gago, and K.A. Friedrich, *Porous Transport Layers for Proton Exchange Membrane Electrolysis Under Extreme Conditions of Current Density, Temperature, and Pressure.* Advanced Energy Materials, 2021. **11**(33): p. 2100630.

70. Razmjooei, F., A. Farooqui, R. Reissner, A.S. Gago, S.A. Ansar, and K.A. Friedrich, *Elucidating the Performance Limitations of Alkaline Electrolyte Membrane Electrolysis: Dominance of Anion Concentration in Membrane Electrode Assembly.* ChemElectroChem, 2020. **7**(19): p. 3951-3960.

71. Janssen, H., J.C. Bringmann, B. Emonts, and V. Schroeder, *Safety-related studies on hydrogen production in high-pressure electrolysers.* International Journal of Hydrogen Energy, 2004. **29**(7): p. 759-770.

72. Cho, M.K., H.-Y. Park, H.J. Lee, H.-J. Kim, A. Lim, D. Henkensmeier, S.J. Yoo, J.Y. Kim, S.Y. Lee, H.S. Park, and J.H. Jang, *Alkaline anion exchange membrane water electrolysis: Effects of electrolyte feed method and electrode binder content.* Journal of Power Sources, 2018. **382**: p. 22-29.

73. Boggs, B.K., R.L. King, and G.G. Botte, *Urea electrolysis: direct hydrogen production from urine.* Chemical Communications, 2009(32): p. 4859-4861.

74. Xu, Z., S. Delgado, V. Atanasov, T. Morawietz, A.S. Gago, and K.A. Friedrich *Novel Pyrrolidinium-Functionalized Styrene-b-ethylene-b-butylene-b-styrene Copolymer Based Anion Exchange Membrane with Flexible Spacers for Water Electrolysis.* Membranes, 2023. **13**, DOI: 10.3390/membranes13030328.

75. Nikolic, J., E. Expósito, J. Iniesta, J. González-Garcia, and V. Montiel, *Theoretical Concepts and Applications of a Rotating Disk Electrode.* Journal of Chemical Education, 2000. **77**(9): p. 1191.

76. Henkensmeier, D., M. Najibah, C. Harms, J. Žitka, J. Hnát, and K. Bouzek, *Overview: State-of-the Art Commercial Membranes for Anion Exchange Membrane Water Electrolysis.* Journal of Electrochemical Energy Conversion and Storage, 2020. **18**(2).

Annex A - Urea Full Oxidation- Intermediate Steps

Table 7.1- Sum of Free Energies for All the intermediate Steps, adapted from [22]

reactions	ΔG (kJ mol^{-1})
$CO(NH_2)_2 + M \rightarrow [M{\cdot}CO(NH_2)_2]_{ads}$	66.2
$[M{\cdot}CO(NH_2)_2]_{ads} + OH^- \rightarrow [M{\cdot}CO(NH_2{\cdot}NH)]_{ads} + H_2O + 1e^-$	−28.9
$[M{\cdot}CO(NH_2)_2{\cdot}NH]_{ads} + OH^- \rightarrow [M{\cdot}CONH_2N]_{ads} + H_2O + 1e^-$	−185.1
$[M{\cdot}CO(NH_2N)]_{ads} + OH^- \rightarrow [M{\cdot}CONHN)]_{ads} + H_2O + 1e^-$	75.4
$[M{\cdot}CONHN]_{ads} + OH^- \rightarrow [M{\cdot}CO{\cdot}N_2]_{ads} + H_2O + 1e^-$	−178.2
$[M{\cdot}CO{\cdot}N_2]_{ads} + OH^- \rightarrow [M{\cdot}CO{\cdot}OH)]_{ads} + N_2 + 1e^-$	392.7
$[M{\cdot}CO{\cdot}OH]_{ads} + OH^- \rightarrow [M{\cdot}CO_2]_{ads} + H_2O + 1e^-$	−156.6
$[M{\cdot}CO_2]_{ads} \rightarrow M + CO_2$	1242.2
total	1227.7

Appendice A Commercially Available Anion Exchange Membranes

Table A.1- Commercially Available Anion Exchange Membranes, properties and prices. Some information is undisclosed. Adapted from [76]

Company	Brand Name	Country	Product names	Ionomr pair	Thickness (μm)	IEC / mmol g^{-1}	Ion conductivity ms cm-1	Water uptake wt %	Comments	Price / $\$\cdot cm^{-2}$
Fumatech	Fumasep®	Germany	FAA-3-30	FumionFAA-3	26-34	1.67 - 2.04	>5 (Cl^-form)	<19	Stability range: pH = 1 – 12 at T = 25 – 50 °C.	0.09-0.21
			FAA-3-50		45-55	1.6 - 2.1	3 – 8 (Cl^-form)	10 – 25	Stability range: pH = 0 - 14 at T = 25 °C.	0.1-0.22
			FAA-3-PK-75		70-80	1.2 – 1.4	4.5 – 6.5 (Cl^- form)	10 – 20	Stability range: pH = 0 - 14 at T = 25 °C.	0.16-0.27
Tokuyama	A201	Japan	A201	na	28	1.39	>2.5 (Cl^-form)	na	na	na
Ionomr	AEMION™	Canada	AF3-HWK9-75-X	AP3-HNN9-00-X	75	1.9-2.7	na	20-50 (OH-)	na	0.4 -1.5
Dioxide Materials	SUSTAINION®	USA	X-37-50	XB-7	50	na	80 (OH- 30 °C)	na	na	0.68 – 2.25
Versogen	PipeION	USA	A70-HCO3	na	70	na	na	na	Stability range: 1 – 14	na
			na	na	80	≈2.35	150 (OH^- 80 °C)	50	Stability range: 1 - 14.	0.34-0.88

Appendice B Nitrogen (N_2) and Oxygen (O_2) purge

During RDE studies, one of the objectives was also to study the influence of an O_2 saturated electrolyte versus a normal N_2 saturated. This could in theory improve ammonia production by inhibit OER and leaving more active sites for U2A conversion to occur. Fig. B.1 shows the results for OXYGEN-N catalyst for AdBlue and AdBlue with 1M KOH.

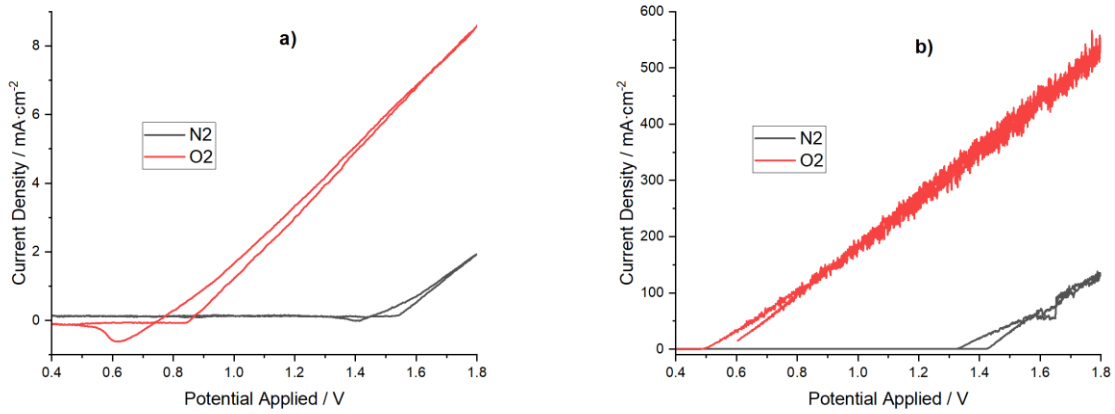

Figure B.1-RDE measurements with support electrolyte solutions purged with either O_2 or N_2. In a), pure AdBlue was used and b) used AdBlue+1 M KOH, both at room temperature

Unfortunately, a shift in the RHE was noticed for experiments with O2 saturated electrolyte. After consulting with the RHE provider, it was concluded that O2 analysis would not be possible with the presented setup since Hydrogen potential depends quite heavily on oxygen dissolved in the electrolyte. To correctly study O_2 influence, a Haber Luggin Capillary should be used to accommodate the RHE.